[32] Hansson L, Lindholm LH, Ekbom T, Dahlof B, Lanke J, Schersten B, et al. Randomised trial of old and new antihypertensive drugs in elderly patients: cardiovascular mortality and morbidity the Swedish Trial in Old Patients with Hypertension-2 study. Lancet 1999;354: 1751–6.

[33] Asano Y, Kim J, Ogai A, Takashima S, Shintani Y, Minamino T, et al. A calcium channel blocker activates both ecto-5(′)-nucleotidase and NO synthase in HUVEC. Biochem Biophys Res Commun 2003; 311:625–8.

[34] Lenasi H, Kohlstedt K, Fichtlscherer B, Mulsch A, Busse R, Fleming I. Amlodipine activates the endothelial nitric oxide synthase by altering phosphorylation on Ser1177 and Thr495. Cardiovasc Res 2003;59:844–53.

ELSEVIER

Cardiovascular Research 67 (2005) 705 – 713

Cardiovascular Research

www.elsevier.com/locate/cardiores

Exacerbation of heart failure in adiponectin-deficient mice due to impaired regulation of AMPK and glucose metabolism

Yulin Liao[a], Seiji Takashima[a], Norikazu Maeda[b], Noriyuki Ouchi[b], Kazuo Komamura[c], Iichiro Shimomura[b], Masatsugu Hori[a], Yuji Matsuzawa[b], Tohru Funahashi[b], Masafumi Kitakaze[c,*]

[a]*Department of Internal Medicine and Therapeutics, Osaka University Graduate School of Medicine, 2-2 Yamadaoka, Suita, Osaka 565-0871, Japan*
[b]*Department of Internal Medicine and Molecular Science, Osaka University Graduate School of Medicine, 2-2 Yamadaoka, Suita, Osaka 565-0871, Japan*
[c]*Cardiovascular Division of Medicine, National Cardiovascular Center, 5-7-1 Fujishirodai, Suita, Osaka 565-8565, Japan*

Received 13 January 2005; received in revised form 5 April 2005; accepted 19 April 2005
Available online 23 May 2005
Time for primary review 24 days

Abstract

Objective: Insulin resistance (IR) was reported to be associated with chronic heart failure (CHF). Adiponectin, an insulin-sensitizing hormone with anti-inflammatory activity, improves energy metabolism via AMP-activated protein kinase (AMPK). AMPK deficiency is associated with depressed cardiac function under stress conditions. However, it is not clear whether adiponectin plays an important role in CHF. We hypothesize that deficiency of adiponectin might result in deterioration of heart failure.
Methods: Using adiponectin null mice and their littermates, we examined the effects of adiponectin on LV pressure overload-induced cardiac hypertrophy and failure, and investigated the mechanisms involved.
Results: Three weeks after transverse aortic constriction (TAC), cardiac hypertrophy (evaluated from the heart-to-body weight ratio: 7.62±0.27 in wild-type (WT) mice, 9.97±1.13 in knockout (KO) mice, $P<0.05$) and pulmonary congestion (lung-to-body weight ratio: 9.05±1.49 in WT mice, 14.95±2.36 in KO mice, $P<0.05$) were significantly greater in adiponectin KO mice than WT mice. LV dimensions were also increased in KO mice. Compared with WT TAC mice, expression of AMPKα protein was lower, while IR was higher in KO TAC mice.
Conclusion: These findings indicate that adiponectin deficiency leads to progressive cardiac remodeling in pressure overloaded condition mediated via lowing AMPK signaling and impaired glucose metabolism.

Keywords: Adiponectin; Heart failure; Myocardial hypertrophy; Metabolic syndrome

1. Introduction

The metabolic syndrome (MetS) has been identified as a constellation of important risk factors for cardiovascular disease (CVD) [1,2]. The Adult Treatment Panel III report (ATP III)[3] identified insulin resistance (IR)±glucose intolerance as an important component of MetS that is related to CVD. Clinical evidence suggests that LV hypertrophy is associated with either impaired glucose tolerance (IGT) or an increase in IR [4]. An increase in IR is also common in CHF patients with either ischemic heart disease or idiopathic dilated cardiomyopathy [5–7]. These findings lead to the concept that a strategy targeting improvement of IGT or IR should be beneficial for cardiac remodeling.

To date, there is compelling evidence that an impaired myocardial energy metabolism strongly influences cardiac remodeling [8–11]. The important role of the AMP-activated protein kinase (AMPK) in cardiac hypertrophy and failure seems to be deserving of more attention. AMPK

* Corresponding author. Tel.: +81 6 6833 5012x2225; fax: +81 6 6836 1120.
E-mail address: kitakaze@zf6.so-net.ne.jp (M. Kitakaze).

0008-6363/$ - see front matter © 2005 European Society of Cardiology. Published by Elsevier B.V. All rights reserved.
doi:10.1016/j.cardiores.2005.04.018

activity and protein expression were both reported to be increased by pressure overload hypertrophy [8], which should be considered a compensatory mechanism for cardiac remodeling, because the overexpression of mutations of this enzyme leads to deterioration of post-ischemic cardiac dysfunction [10] or experimental glycogen storage cardiomyopathy [11]. Accordingly, we considered that AMPK might play an important role in limiting cardiac remodeling and that an increase of AMPK in the heart might inhibit remodeling by regulation of cellular metabolism to maintain energy homeostasis under stress conditions. Intriguingly, adiponectin, an endogenous adipocyte-derived insulin-sensitizing hormone, has been shown to attenuate inflammation, regulate glucose and lipid metabolism. In addition, adiponectin is able to stimulate glucose utilization and fatty acid oxidation through the activation of AMPK [12]. Furthermore, administration of adiponectin reverses IR in mice with lipoatrophy and diabetes [13,14]. The importance of adiponectin has also been demonstrated by other evidence that it may directly influence the development of cardiovascular disease [15–17]. A recent clinical investigation demonstrated that a high plasma adiponectin concentration was associated with a lower risk of myocardial infarction in men [17]. These lines of evidence strongly suggest that adiponectin might play an important role in the inhibition of cardiac remodeling via its beneficial effects on MetS. Interestingly, a recent experimental study shows that 1 week pressure overload in adiponectin-deficient mice resulted in enhanced concentric cardiac hypertrophy with an increased mortality [18]. However, to our knowledge, no previous study has evaluated the role of AMPK or adiponectin on chronic heart failure (CHF). Therefore, we aimed to test the hypothesis that adiponectin might act as an endogenous protective modulator of chronic cardiac remodeling via regulation of AMPK.

In this study, we evaluated the role of adiponectin in the progression of cardiac hypertrophy and heart failure in a model of LV pressure overload using adiponectin knockout mice, and explored the potential mechanisms involved.

2. Methods

2.1. Adiponectin knockout (KO) mice

Adiponectin KO mice were generated as described previously [19]. Wild-type (WT) littermates served as the control.

2.2. TAC model

All procedures were performed in accordance with our institutional guidelines for animal research and comply with the Declaration of Helsinki and the NIH Guide. Mice (male, 9–10 weeks old, wt 25–29 g) were anesthetized with a mixture of xylazine (5 mg/kg) and ketamine (100 mg/kg, i.p.), and transverse aortic constriction (TAC) was created as we described previously. In order to confirm that pressure overload was similar between the wild-type and the KO mice, three mice in each group were selected for measurement of the ascending aortic pressure using a 1.4 F Millar pressure catheter on the second day after TAC. The other mice were killed after 3 weeks for morphological analysis. Mice were divided into four groups: WT sham ($n=5$), WT TAC ($n=24$), KO sham ($n=5$), and KO TAC ($n=24$).

2.3. Histology

Hearts were fixed with 10% formalin. The cardiac myocyte cross-sectional surface area was measured using three hearts in each group after images were captured from HE-stained sections as described elsewhere [20]. One hundred myocytes per heart were counted, and the average area was determined. Myocardial and perivascular fibrosis were stained with Azan [21].

2.4. Echocardiography

Transthoracic echocardiography was performed with a Sonos 4500 and a 15–6 L MHz transducer (Philips, the Netherlands). Mice were fixed while conscious and good two-dimensional short-axis LV views were obtained for guided M-mode measurements of the LV posterior wall thickness (LVPW), LV end-diastolic diameter (LVEDd), LV end-systolic diameter (LVESd), LV fractional shortening (LVFS), and LV ejection fraction (EF). $LVFS=(LVEDd-LVESd)/LVEDd*100$, $LVEF=[(LVEDd)^3-(LVESd)^3]/(LVEDd)^3*100$.

2.5. Measurement of glucose and insulin

Fasting plasma glucose was measured using a blood glucose test meter (Glutestace GT-1640, Arkray Company, Japan). After 14 h withdrawal of food from the cages, whole blood sample (3 μl) was taken from mouse tails with a glucose sensor inserted in Glutestace, and the result of plasma glucose concentration was read-out 30 s later. Serum insulin levels were measured according to the protocols of the manufacturers (EIA-3440 ELISA kit, DRG, German). IR was assessed with the homeostasis model: HOMA-IR = fasting glucose level (mg/dl) × fasting insulin level (ng/ml) ÷ 22.5.

2.6. Western blot analysis

SDS-PAGE was performed with 50 μg of protein extracted from mouse hearts. Blots were incubated with a mouse monoclonal antibody directed against anti-AMPKα_1, anti-AMPKα_2 antibodies (upstate). Signals obtained by Western blotting were quantified using Scion Image software.

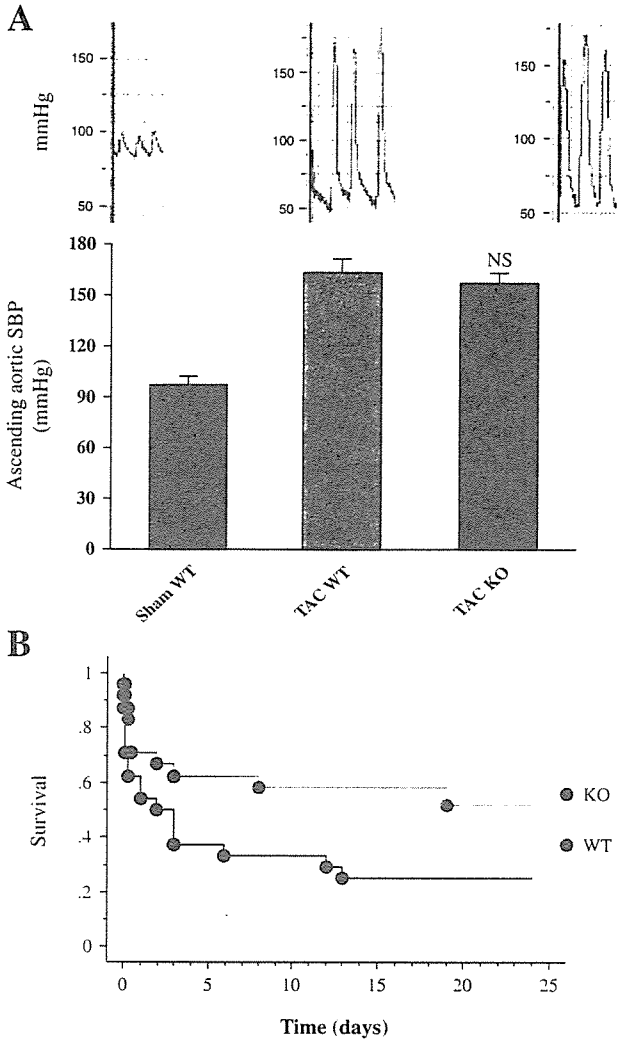

Fig. 1. Left ventricular pressure overload and survival. A) The ascending aortic systolic pressure measured with a 1.4 F catheter was similar in adiponectin KO and WT mice. NS: not significant vs. TAC WT. B) Kaplan–Meier survival analysis showed a significant higher mortality in adiponectin KO mice after TAC (Mantel–Cox test: $P=0.031$, $n=24$ in both WT and KO groups).

2.7. Statistical analysis

For all statistical tests, multiple comparisons were performed by one-way ANOVA with the Tukey–Kramer exact probability test. Survival analysis was performed using the Kaplan–Meier method. Variables with skewed distribution were transformed to logarithmic data. Results are reported as the mean ± SEM and $P<0.05$ was considered statistically significant.

3. Results

3.1. LV pressure overload and survival

To evaluate the role of adiponectin in cardiac remodeling, we used mice lacking the adiponectin/*CRP30* gene. During development up to 16 weeks of age, there were no differences in growth rate and food intake between WT mice and KO (homozygous) mice [19]. The results showed that LV pressure overload was similar in WT and KO mice (Fig. 1A). The mortality after TAC was significantly higher in KO mice than WT mice (Fig. 1B). We found that acute or subacute heart failure was the main cause of death confirmed by postmortem examination (pulmonary edema or hemorrhage was noted in most of the dead mice. Lung-to-body weight ration was 13.1 ± 2.3 mg/g for dead mice in adiponectin KO mice, 11.4 ± 1.9 mg/g for dead mice in WT group). Body weight (BW) and blood pressure (determined by tail cuff measurement) were similar before TAC (BW: 27.1 ± 0.4 g in KO, 27.7 ± 0.4 g in WT) and 3 weeks after TAC (BW: 24.5 ± 1.4 g in KO, 25.5 ± 0.7 g in WT).

3.2. Earlier transition from hypertrophy to heart failure in KO mice

Serial echocardiographic examinations showed that the heart function evaluated by LVEF and LVFS progressively

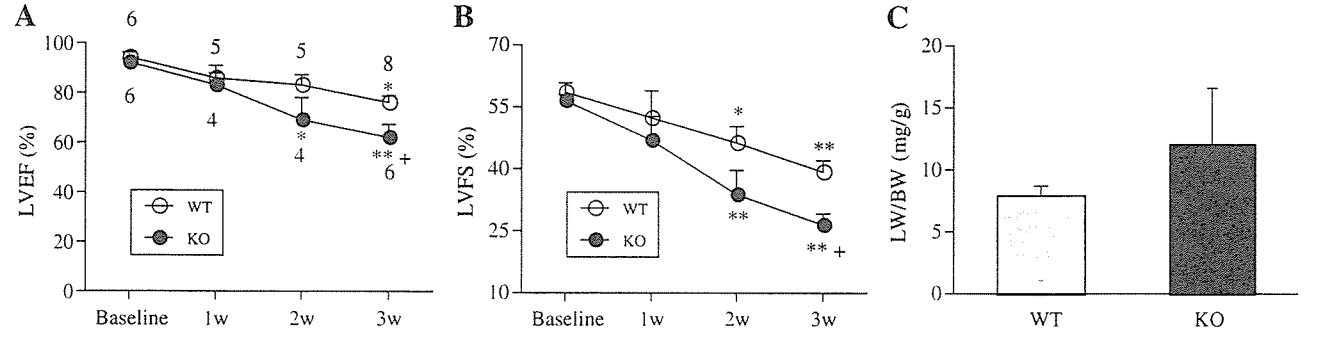

Fig. 2. The transition from hypertrophy to heart failure. A) Left ventricular ejection fraction (LVEF) and B) left ventricular fractional shortening (LVFS) were progressively depressed in adiponectin KO mice after 1 week of TAC, and the transition to heart failure occurred at 2 weeks after TAC in KO mice, which was confirmed by sacrifice to show an significant increase of lung-to-body weight ratio (C, $n=4$ for both WT and TAC mice). The number of mice in each time point for echocardiographic examination is indicated above or under the data points. $^{*}P<0.05$, $^{**}P<0.01$ vs. baseline, $\dagger P<0.05$ vs. WT mice.

depressed in both adiponectin KO and WT mice over the course of 3 weeks (Fig. 2A, B). Two weeks after TAC, a significant reduction of LVEF and LVFS was noted in KO mice, indicating a proceeded transition to heart failure. To confirm the occurrence of heart failure, we sacrificed four mice in both KO and WT groups at 2 weeks after TAC and found a marked pulmonary congestion in KO mice (Fig. 2C).

3.3. Greater cardiac hypertrophy in KO mice

Three weeks after TAC, mice were sacrificed after echocardiographic examination. The wet heart-to-body weight ratio (HW/BW) was increased by 53% in TAC WT mice compared with sham WT mice, whereas HW/BW was dramatically increased by 110% in adiponectin TAC KO mice vs. sham KO mice. There was a significant difference of HW/BW between WT and KO TAC mice (Fig. 3A–C, E). The cross-sectional surface area of cardiac myocytes was significantly larger in KO mice than WT mice (Fig. 3F). There were no significant differences of HW/BW and cardiac myocyte cross-sectional surface area between WT and KO sham mice. These findings indicate that cardiac hypertrophy was far more extensive in adiponectin KO mice. We also examined myocardial and perivascular fibrosis and did not find significant difference between WT and KO TAC mice (Fig. 3D).

3.4. Worse pulmonary congestion in KO mice

We confirmed in previous studies that pulmonary edema is a reliable index of cardiac function in this model [22–24]. Severe pulmonary congestion was found in adiponectin KO mice. Compared with sham mice, the lung-to-body weight ratio (LW/BW) was increased by 170% in KO TAC mice,

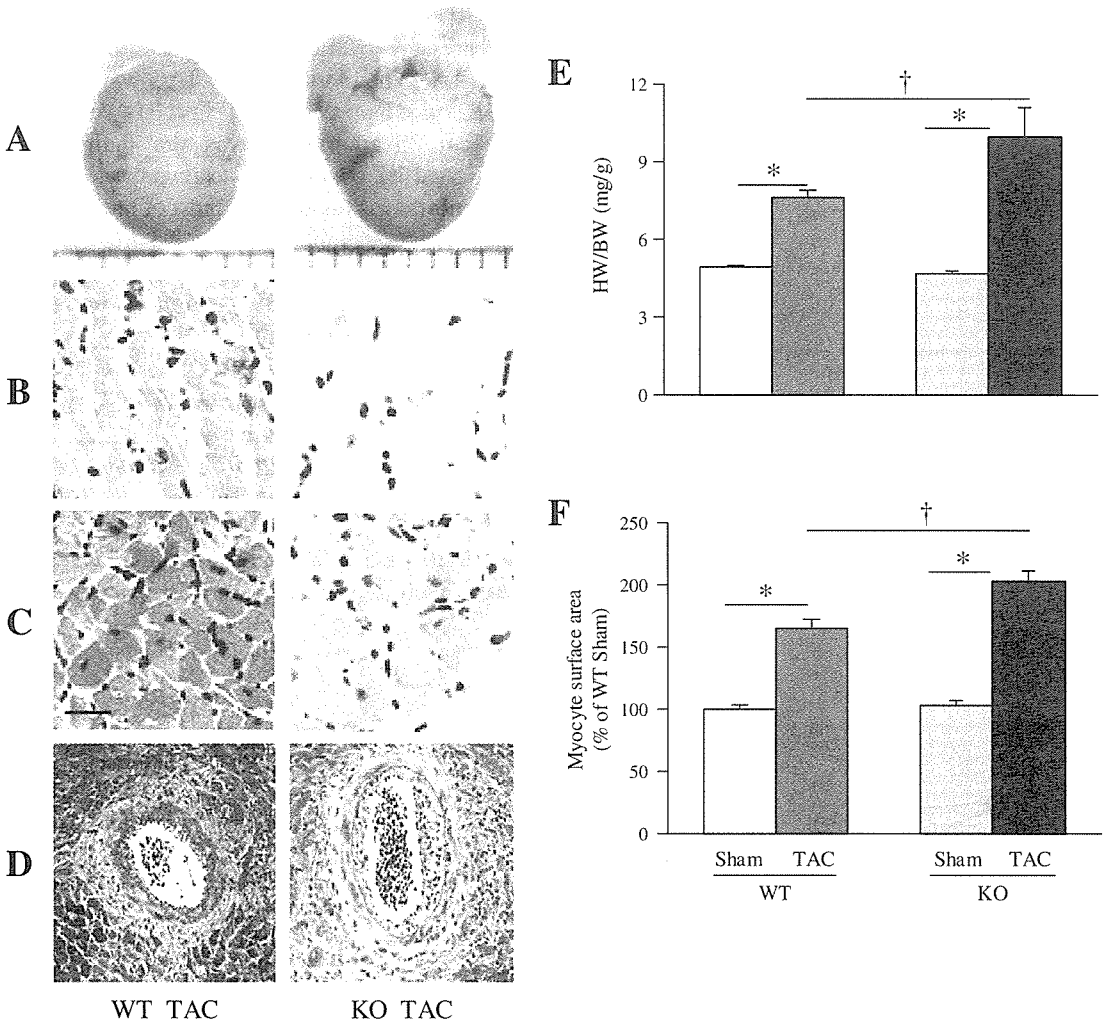

Fig. 3. Cardiac remodeling was more severe in KO mice. A) Representative pictures of cardiac hypertrophy in WT and KO mice at 3 weeks after TAC. B and C) Represent long-axis and cross-sectional views of cardiac myocytes with HE staining. D) Represents cardiac fibrosis with Azan staining (×100 magnification). HW/BW (E, $n=5$ in both sham groups, $n=8$ in WT TAC group, and $n=6$ in KO TAC group) and the cardiac myocyte cross-sectional surface area (F, $n=2$ in each sham group and $n=3$ in each TAC group) were increased significantly in KO mice compared with their wild-type (WT) littermates. *$P<0.01$, †$P<0.05$. Bar=20 μm for B and C.

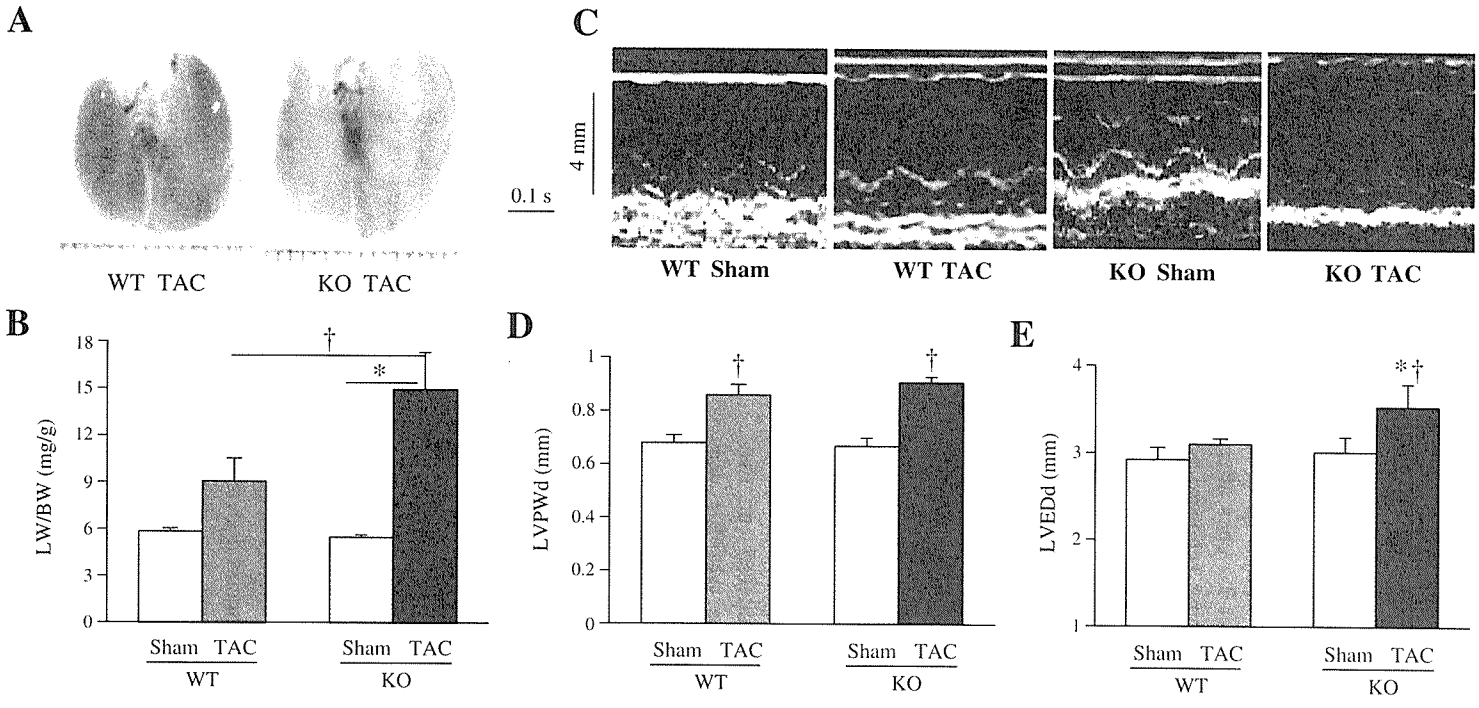

Fig. 4. Pulmonary congestion and echocardiographic findings at 3 weeks after TAC. The lungs of an adiponectin KO mouse were markedly enlarged compared with those of WT mice (A). The lung-to-body weight ratio (LW/BW) was markedly increased in KO mice compared with WT mice (B). $*P<0.01$, $\dagger P<0.05$. Echocardiography (C) shows that the LV posterior wall diastolic thickness (LVPWd) (D) is similar in KO and WT TAC mice. The LV end-diastolic dimension (LVEDd) (E) is significantly increased in KO mice compared with WT mice $*P<0.05$ vs. TAC WT. $\dagger P<0.01$ vs. responding sham mice. The number of animals is the same as Fig. 3 in each group for analysis of LW/BW and echocardiography.

whereas there was only a 55% increase in WT TAC littermates (Fig. 4A, B). There was no significant difference in LW/BW between KO and WT sham mice. We did not evaluate LV hemodynamics using a Millar pressure catheter because most of the KO mice appeared to be too weak to endure this procedure (including anesthesia) at 3 weeks after TAC.

3.5. Echocardiography findings

Because anesthesia has a significant influence on echocardiography data in mice [25] and most of the KO TAC mice were too weak for anesthesia at 3 weeks after TAC, we developed a method of performing echocardiographic examination in conscious mice. Compared with WT TAC mice, there was a significant decrease in both LV fractional shortening (LVFS) and the LV ejection fraction (LVEF) in KO TAC mice (Fig. 2A, B), and marked LV chamber dilation was observed in KO TAC mice (Fig. 4C, D). In contrast, there were no significant differences in these parameters between WT sham and KO sham mice. These findings indicate an increase in cardiac remodeling under pressure overload in adiponectin KO mice.

3.6. Myocardial AMPK expression

AMPK consists of one catalytic subunit (α) and two noncatalytic subunits (β and γ). Because AMPKα was reported to be activated by adiponectin [12], we examined the AMPKα_1 and α_2 protein expression in the hearts of WT and KO mice. As shown in Fig. 5, in the presence of LV pressure overload, AMPKα expression increased significantly, but the increment of AMPKα protein was less in KO than in WT hearts. These findings suggested that adiponectin deficiency means that the expression of AMPK cannot be increased sufficiently enough to provide adequate cardiac protection under stress conditions.

3.7. Increase of fasting glucose and IR

As IR is closely associated with cardiac remodeling [4–7] and adiponectin deficiency can lead to diet-induced IR [19], we determined the influence of adiponectin deficiency on glucose metabolism and IR in mice with LV pressure overload. As shown in Fig. 6A, fasting glucose levels increased by 40% in KO mice at 3 weeks after TAC, but rose by only about 20% in WT littermates, suggesting that the glucose metabolisms were more impaired in the adiponectin KO mice. Meanwhile, a similar increase in serum insulin was noted in both WT and KO TAC mice (Fig. 6B). As an index of IR, HOMA-IR was more increased, in adiponectin KO mice than in WT mice at three weeks after TAC (Fig. 6C). Furthermore, we found a significant positive correlation between IR and the heart weight-to-body weight ratio in adiponectin KO mice rather than in WT mice (Fig. 6D), indicating that IR might also be involved in cardiac remodeling in adiponectin KO mice.

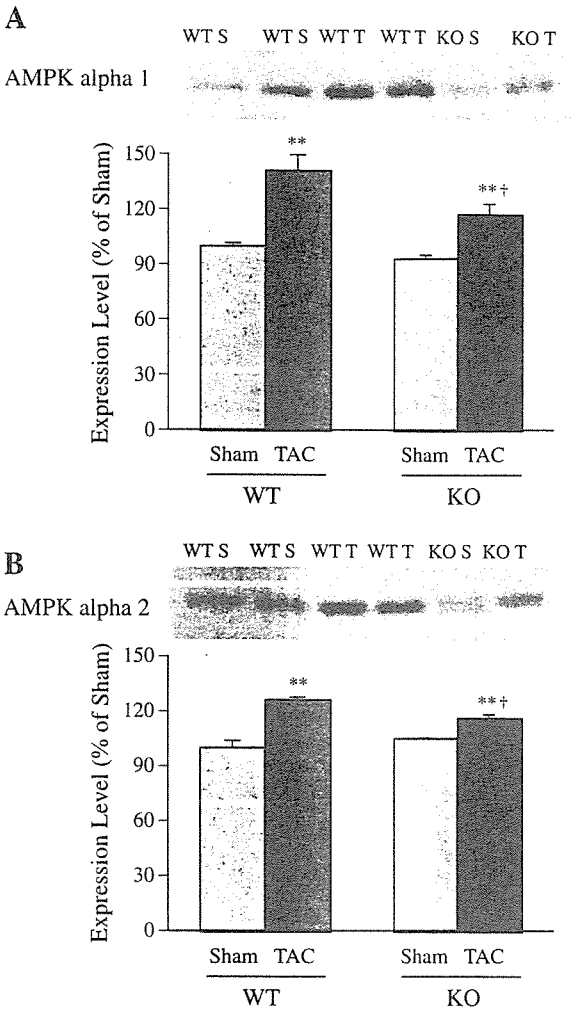

Fig. 5. Myocardial expression of AMPK. AMPKα_1 (A), α_2 (B) were increased in TAC mice, but the change was smaller in KO mice ($n=3$ in each group, $^{**}P<0.01$ vs. responding sham mice; $\dagger P<0.05$ vs. WT TAC). S: sham, T: TAC.

4. Discussion

In this study, we found that adiponectin deficiency worsens cardiac remodeling induced by LV pressure overload, and this change was associated closely with a decrease in the expression of AMPK, and an increase in IR. These results are consistent with a recent study by Shibata et al. [18] showing that pressure overload for one week in adiponectin KO mice resulted in greater cardiac hypertrophy and higher mortality. Differently, this study further investigated the potential role of adiponectin-deficiency on the development of cardiac hypertrophy and chronic heart failure. We demonstrated that the transition from hypertrophy to heart failure proceeded in adiponectin KO mice. Additionally, we investigated the influence of adiponectin

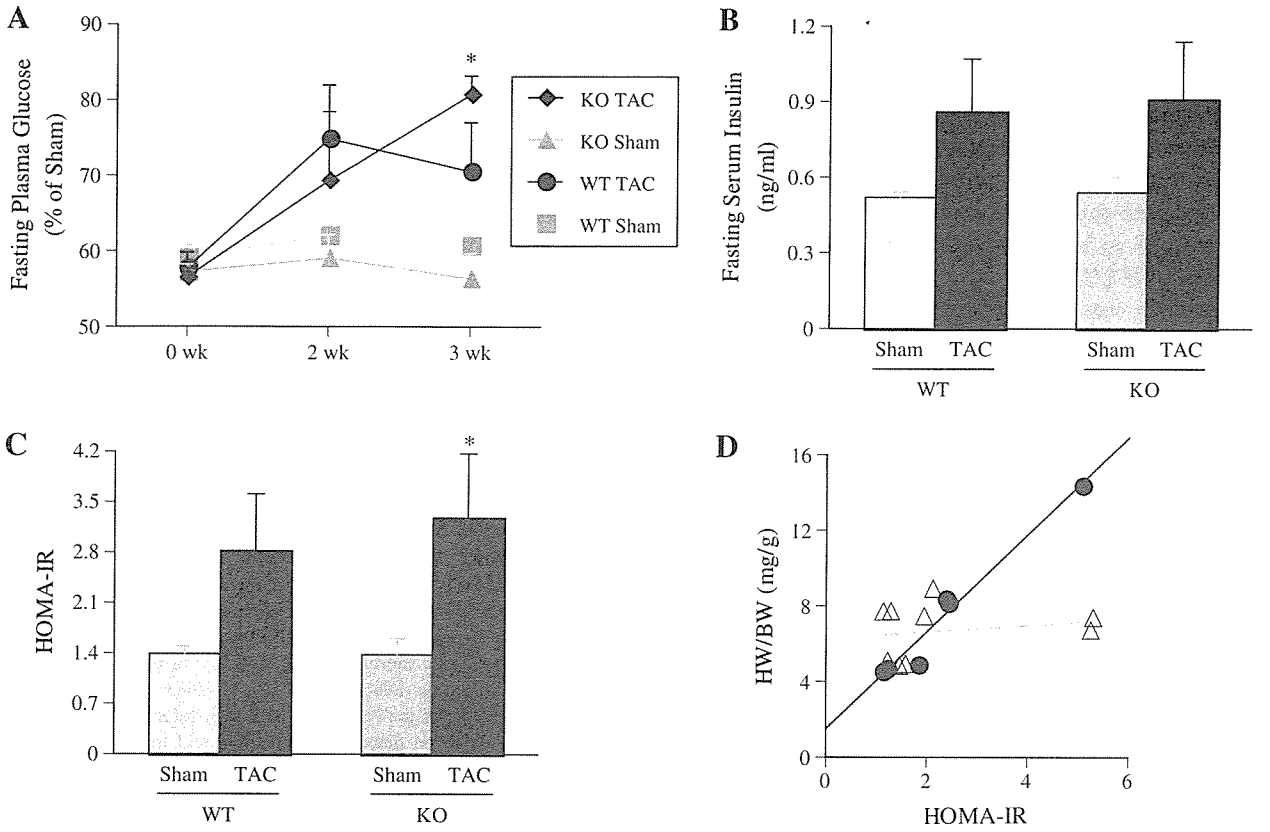

Fig. 6. Changes in glucose metabolism. Fasting glucose levels (A) were increased in adiponectin KO mice at 3 weeks after the onset of TAC, $*P<0.01$ vs. WT TAC ($n=5$ for all the groups at 0 week and for both sham groups at other two time points; $n=4$ for WT and KO TAC mice at 2 weeks, and $n=5$ and 3 for WT and KO TAC mice at 3 weeks, respectively). Serum insulin (B) was increased after TAC, but no significant difference was found between WT and KO mice, while the insulin resistance index HOMA-IR (C) was increased in KO mice. $\dagger P<0.05$ vs. KO sham ($n=3$ in both KO sham and TAC groups, $n=3$ in WT sham and $n=6$ in TAC groups). Linear correlation between HOMA-IR and HW/BW in both WT and KO mice groups (D) irrespective of TAC, $r=0.982$, $P<0.0001$, $n=6$ for KO mice (solid circle), while no significant correlation was found for WT mice ($n=9$, open triangle).

on glucose metabolism and addressed the important relation between metabolism and cardiac remodeling.

An increase in IR, glucose intolerance, and a proinflammatory state are among the six components of the MetS related to CVD, which is viewed as the primary outcome of this syndrome. In the present study, we noted that adiponectin deficiency induced an increase in IR and fasting glucose levels in the presence of pressure overload, suggesting that adiponectin has a strong influence on MetS and subsequently on cardiac remodeling. An increase in IR appears to downregulate adiponectin receptor expression via the phosphoinositide 3-kinase/Foxo1-dependent pathway [26]. In addition, Foxo1 is recognized as a negative regulator of insulin sensitivity [27], so it is theoretically acceptable that adiponectin knockout leads to MetS or that adiponectin KO mice are more susceptible to MetS under pathological stress. Although the exact relationship between MetS and CVD is not clear, both genetic and environmental factors may be involved. There is evidence that neuroendocrine factors [28] or the RAS (review [29]) may play an important role in MetS. We previously showed that plasma concentrations of catecholamines and renin were increased by LV pressure overload in mice [23]. In the present study, in addition to endogenous adiponectin deficiency, activation of the sympathoadrenal system and renin–angiotensin system (RAS) may have contributed to the onset of MetS.

The impact of MetS on CVD mortality has been investigated in several clinical studies [30–32]. It is generally agreed that CVD mortality is higher in subjects with MetS than in those without it. We found a positive correlation between IR and cardiac hypertrophy in adiponectin KO mice rather than in WT mice in this study, with both IR and HW/BW higher in adiponectin KO mice than in WT mice, suggesting that deficiency of adiponectin contributed to enhanced cardiac remodeling. Consistent with our results, a recent case-control study found that abnormal LV geometry and LV dysfunction were related to MetS [33]. Additionally, it is well known that type 2 diabetic patients are susceptible to diabetic cardiomyopathy, and the fasting plasma insulin level was reported to be the strongest independent predictor of LV mass in type 2 diabetes [34]. Taken together, these findings support the concept that MetS has an impact on cardiac remodeling. Although IR is known to be an important contributor to the

progression of heart failure, our data reported here are not enough to delineate the causal relationship between IR and cardiac remodeling. In spite of an increase tendency of IR showing in mice with cardiac hypertrophy, we did not find a significant correlation between IR and heart-to-body weight ratio in a relatively small sample of wild-type mice. In accordance with this study, previous clinical observations have shown IR to be related to the thickness of LV walls rather than LVH [35,36].

Adiponectin was reported to reduce the production of TNFα, and to improve both glucose metabolism and IR via the AMPK signaling pathway [12], suggesting that it may improve MetS. Evidence is emerging to demonstrate a critical role of AMPK in cardiac remodeling. Mutation of the gamma 2 subunit of AMPK has been shown to cause glycogen storage cardiomyopathy, and the influence of AMPKα on cardiac remodeling is another attractive research field. Both AMPKα_1 and AMPKα_2 expression were increased in hypertrophied hearts in the present study, which is only partially consistent with a previous investigation by Tian et al. [8]. They reported that α_1 was increased, α_2 expression was decreased, whereas activity of both AMPKα_1 and α_2 was increased in pressure overload rats. The reasons for this discrepancy are not clear. Generally, the activity of both AMPKα_1 and α_2 was reported to increase under stress conditions such as ischemia and pressure overload [8,10,18]. The protein expression of myocardial AMPK was seldom investigated and the reports are inconsistent. Acute ischemia [37] or short-term pressure overload [18] stimulates activity of myocardial AMPK without changing the AMPK protein expression, whereas both AMPKα_2 activity and expression were decreased at three weeks following volume-overload [38]. AMPK deficiency is reported to result in depressed LV function, increased myocardial necrosis, and apoptosis following ischemia/reperfusion injury [10]. The finding that AMPKα protein expression was increased in WT mice after TAC suggests that the augmentation of AMPKα signaling is a compensatory mechanism that attempts to maintain energy homeostasis in the heart under pressure overload. This mechanism may be partly controlled by adiponectin, because AMPK signaling was impaired in adiponectin KO mice and there was consequent progression of cardiac remodeling. Thus, this study provided a new link between adiponectin and AMPK in the process of cardiac remodeling. Apart from its influence on IR, AMPK, and TNFα, other mechanisms may also be involved in the beneficial effect of adiponectin on cardiac remodeling. Adiponectin has been reported to suppress superoxide generation and enhance eNOS activity [39], to have an antiproliferative effect [40], and to counteract beta adrenergic stimulation [41], all of which are closely related to cardiac remodeling [42]. Interestingly, AMPK and eNOS co-localize in hearts and AMPK was reported to activate eNOS [43,44]. Thus, it is reasonable for adiponectin deficiency to lead to progressive cardiac remodeling in response to pressure overload, as we showed in this study.

Acknowledgments

We thank Dr. Hidetoshi Okazaki, Hui Zhao and Dr Masakatsu Wakeno for their technical assistance. This work was supported by Grants (H13-Genome-011, H13-21seiki (seikatsu)-23) from the Ministry of Health, Labor and Welfare, Japan. Dr Liao is supported by a grant from the Japan Society for the Promotion of Science (P05228).

References

[1] Rutter MK, Meigs JB, Sullivan LM, D'Agostino RB, Wilson Sr. PW. C-reactive protein, the metabolic syndrome, and prediction of cardiovascular events in the Framingham Offspring Study. Circulation 2004;110:380–5.
[2] Isomaa B, Almgren P, Tuomi T, Forsen B, Lahti K, Nissen M, et al. Cardiovascular morbidity and mortality associated with the metabolic syndrome. Diabetes Care 2001;24:683–9.
[3] Third report of the National Cholesterol Education Program (NCEP) expert panel on detection, evaluation, and treatment of high blood cholesterol in adults (Adult Treatment Panel III) final report. Circulation 2002;106:3143–421.
[4] Rutter MK, Parise H, Benjamin EJ, Levy D, Larson MG, Meigs JB, et al. Impact of glucose intolerance and insulin resistance on cardiac structure and function: sex-related differences in the Framingham Heart Study. Circulation 2003;107:448–54.
[5] Swan JW, Anker SD, Walton C, Godsland IF, Clark AL, Leyva F, et al. Insulin resistance in chronic heart failure: relation to severity and etiology of heart failure. J Am Coll Cardiol 1997;30:527–32.
[6] Paolisso G, De Riu S, Marrazzo G, Verza M, Varricchio M, D'Onofrio F. Insulin resistance and hyperinsulinemia in patients with chronic congestive heart failure. Metabolism 1991;40:972–7.
[7] Kemppainen J, Tsuchida H, Stolen K, Karlsson H, Bjornholm M, Heinonen OJ, et al. Insulin signalling and resistance in patients with chronic heart failure. J Physiol 2003;550:305–15.
[8] Tian R, Musi N, D'Agostino J, Hirshman MF, Goodyear LJ. Increased adenosine monophosphate-activated protein kinase activity in rat hearts with pressure-overload hypertrophy. Circulation 2001;104:1664–9.
[9] Asakawa M, Takano H, Nagai T, Uozumi H, Hasegawa H, Kubota N, et al. Peroxisome proliferator-activated receptor gamma plays a critical role in inhibition of cardiac hypertrophy in vitro and in vivo. Circulation 2002;105:1240–6.
[10] Russell III RR, Li J, Coven DL, Pypaert M, Zechner C, Palmeri M, et al. AMP-activated protein kinase mediates ischemic glucose uptake and prevents postischemic cardiac dysfunction, apoptosis, and injury. J Clin Invest 2004;114:495–503.
[11] Arad M, Moskowitz IP, Patel VV, Ahmad F, Perez-Atayde AR, Sawyer DB, et al. Transgenic mice overexpressing mutant PRKAG2 define the cause of Wolff–Parkinson–White syndrome in glycogen storage cardiomyopathy. Circulation 2003;107:2850–6.
[12] Yamauchi T, Kamon J, Minokoshi Y, Ito Y, Waki H, Uchida S, et al. Adiponectin stimulates glucose utilization and fatty-acid oxidation by activating AMP-activated protein kinase. Nat Med 2002;8:1288–95.
[13] Yamauchi T, Kamon J, Waki H, Terauchi Y, Kubota N, Hara K, et al. The fat-derived hormone adiponectin reverses insulin resistance associated with both lipoatrophy and obesity. Nat Med 2001;7:941–6.
[14] Berg AH, Combs TP, Du X, Brownlee M, Scherer PE. The adipocyte-secreted protein Acrp30 enhances hepatic insulin action. Nat Med 2001;7:947–53.

[15] Funahashi T, Nakamura T, Shimomura I, Maeda K, Kuriyama H, Takahashi M, et al. Role of adipocytokines on the pathogenesis of atherosclerosis in visceral obesity. Intern Med 1999;38:202–6.
[16] Takahashi M, Arita Y, Yamagata K, Matsukawa Y, Okutomi K, Horie M, et al. Genomic structure and mutations in adipose-specific gene, adiponectin. Int J Obes Relat Metab Disord 2000;24:861–8.
[17] Pischon T, Girman CJ, Hotamisligil GS, Rifai N, Hu FB, Rimm EB. Plasma adiponectin levels and risk of myocardial infarction in men. Jama 2004;291:1730–7.
[18] Shibata R, Ouchi N, Ito M, Kihara S, Shiojima I, Pimentel DR, et al. Adiponectin-mediated modulation of hypertrophic signals in the heart. Nat Med 2004;10:1384–9.
[19] Maeda N, Shimomura I, Kishida K, Nishizawa H, Matsuda M, Nagaretani H, et al. Diet-induced insulin resistance in mice lacking adiponectin/ACRP30. Nat Med 2002;8:731–7.
[20] Sanada S, Node K, Minamino T, Takashima S, Ogai A, Asanuma H, et al. Long-acting Ca2+ blockers prevent myocardial remodeling induced by chronic NO inhibition in rats. Hypertension 2003;41: 963–7.
[21] Liao Y, Asakura M, Takashima S, Ogai A, Asano Y, Asanuma H, et al. Benidipine, a long-acting calcium channel blocker, inhibits cardiac remodeling in pressure-overloaded mice. Cardiovasc Res 2005;65: 879–88.
[22] Liao Y, Ishikura F, Beppu S, Asakura M, Takashima S, Asanuma H, et al. Echocardiographic assessment of LV hypertrophy and function in aortic-banded mice: necropsy validation. Am J Physiol Heart Circ Physiol 2002;282:H1703–8.
[23] Liao Y, Takashima S, Asano Y, Asakura M, Ogai A, Shintani Y, et al. Activation of adenosine A1 receptor attenuates cardiac hypertrophy and prevents heart failure in murine left ventricular pressure-overload model. Circ Res 2003;93:759–66.
[24] Liao Y, Asakura M, Takashima S, Ogai A, Asano Y, Shintani Y, et al. Celiprolol, a vasodilatory beta-blocker, inhibits pressure overload-induced cardiac hypertrophy and prevents the transition to heart failure via nitric oxide-dependent mechanisms in mice. Circulation 2004;110: 692–9.
[25] Roth DM, Swaney JS, Dalton ND, Gilpin EA, Ross Jr J. Impact of anesthesia on cardiac function during echocardiography in mice. Am J Physiol Heart Circ Physiol 2002;282:H2134–40.
[26] Tsuchida A, Yamauchi T, Ito Y, Hada Y, Maki T, Takekawa S, et al. Insulin/Foxo1 pathway regulates expression levels of adiponectin receptors and adiponectin sensitivity. J Biol Chem 2004;279:30817–22.
[27] Nakae J, Biggs III WH, Kitamura T, Cavenee WK, Wright CV, Arden KC, et al. Regulation of insulin action and pancreatic beta-cell function by mutated alleles of the gene encoding forkhead transcription factor Foxo1. Nat Genet 2002;32:245–53.
[28] Brunner EJ, Hemingway H, Walker BR, Page M, Clarke P, Juneja M, et al. Adrenocortical, autonomic, and inflammatory causes of the metabolic syndrome: nested case-control study. Circulation 2002;106: 2659–65.
[29] Prasad A, Quyyumi AA. Renin–angiotensin system and angiotensin receptor blockers in the metabolic syndrome. Circulation 2004;110: 1507–12.
[30] Malik S, Wong ND, Franklin SS, Kamath TV, L'Italien GJ, Pio JR, et al. Impact of the metabolic syndrome on mortality from coronary heart disease, cardiovascular disease, and all causes in United States adults. Circulation 2004;110:1245–50.
[31] Trevisan M, Liu J, Bahsas FB, Menotti A. Syndrome X and mortality: a population-based study. Risk factor and life expectancy research group. Am J Epidemiol 1998;148:958–66.
[32] Lakka HM, Laaksonen DE, Lakka TA, Niskanen LK, Kumpusalo E, Tuomilehto J, et al. The metabolic syndrome and total and cardiovascular disease mortality in middle-aged men. Jama 2002;288:2709–16.
[33] Chinali M, Devereux RB, Howard BV, Roman MJ, Bella JN, Liu JE, et al. Comparison of cardiac structure and function in American Indians with and without the metabolic syndrome (the Strong Heart Study). Am J Cardiol 2004;93:40–4.
[34] de Kreutzenberg SV, Avogaro A, Tiengo A, Del Prato S. Left ventricular mass in type 2 diabetes mellitus. A study employing a simple ECG index: the Cornell voltage. J Endocrinol Invest 2000;23: 139–44.
[35] Sundstrom J, Lind L, Nystrom N, Zethelius B, Andren B, Hales CN, et al. Left ventricular concentric remodeling rather than left ventricular hypertrophy is related to the insulin resistance syndrome in elderly men. Circulation 2000;101:2595–600.
[36] Paolisso G, Galderisi M, Tagliamonte MR, de Divitis M, Galzerano D, Petrocelli A, et al. Myocardial wall thickness and left ventricular geometry in hypertensives. Relationship with insulin. Am J Hypertens 1997;10:1250–6.
[37] Altarejos JY, Taniguchi M, Clanachan AS, Lopaschuk GD. Myocardial ischemia differentially regulates LKB1 and an alternate 5′-AMP-activated protein kinase kinase. J Biol Chem 2005;280:183–90.
[38] Kantor PF, Robertson MA, Coe JY, Lopaschuk GD. Volume overload hypertrophy of the newborn heart slows the maturation of enzymes involved in the regulation of fatty acid metabolism. J Am Coll Cardiol 1999;33:1724–34.
[39] Motoshima H, Wu X, Mahadev K, Goldstein BJ. Adiponectin suppresses proliferation and superoxide generation and enhances eNOS activity in endothelial cells treated with oxidized LDL. Biochem Biophys Res Commun 2004;315:264–71.
[40] Brakenhielm E, Veitonmaki N, Cao R, Kihara S, Matsuzawa Y, Zhivotovsky B, et al. Adiponectin-induced antiangiogenesis and antitumor activity involve caspase-mediated endothelial cell apoptosis. Proc Natl Acad Sci U S A 2004;101:2476–81.
[41] Fasshauer M, Klein J, Neumann S, Eszlinger M, Paschke R. Adiponectin gene expression is inhibited by beta-adrenergic stimulation via protein kinase A in 3T3-L1 adipocytes. FEBS Lett 2001; 507:142–6.
[42] Grundy SM, Brewer Jr HB, Cleeman JI, Smith Jr SC, Lenfant C. Definition of metabolic syndrome: report of the National Heart, Lung, and Blood Institute/American Heart Association conference on scientific issues related to definition. Circulation 2004;109:433–8.
[43] Li J, Hu X, Selvakumar P, Russell III RR, Cushman SW, Holman GD, et al. Role of the nitric oxide pathway in AMPK-mediated glucose uptake and GLUT4 translocation in heart muscle. Am J Physiol Endocrinol Metab 2004;287:E834–41.
[44] Chen ZP, Mitchelhill KI, Michell BJ, Stapleton D, Rodriguez-Crespo I, Witters LA, et al. AMP-activated protein kinase phosphorylation of endothelial NO synthase. FEBS Lett 1999;443:285–9.

Circ J 2005; **69:** 243–245

Cardiac Tumor as an Initial Manifestation of Acquired Immunodeficiency Syndrome

Noriaki Iwahashi, MD; Satoshi Nakatani, MD; Hiroyuki Kakuchi, MD; Masakazu Yamagishi, MD; Kazuki Fukuchi, MD*; Yoshio Ishida, MD*; Keiji Hirooka, MD†; Yukihiro Koretsune, MD†; Chisato Ueta, MD‡; Takuma Shirasaka, MD‡; Masafumi Kitakaze, MD

A cardiac tumor was the first manifestation of acquired immunodeficiency syndrome (AIDS) in a female patient in a state of severe immunodeficiency caused by human immunodeficiency virus (HIV) infection. The extensive cardiac and extracardiac involvement shown by various imaging modalities, including echocardiography and ^{18}F-fluorodeoxyglucose positron emission tomography (FDG-PET), suggested that she was in the critical stage of non-Hodgkin's lymphoma (NHL). AIDS was treated by highly active-antiretroviral therapy and the NHL was treated by a combination of rituximab–cyclophosphamide–vincristine–doxorubicine–predonisolone. After 6 cycles of chemotherapy, she was in complete remission. Her cardiac tumor dramatically reduced in size and FDG-PET showed no positive uptake on whole body imaging. Generally, an AIDS-related cardiac tumor tends to be diagnosed at the late stage of the disease because of its nonspecific clinical findings, resulting in an extremely poor prognosis. In the present case, the cardiac tumor was detected by echocardiography and treated with appropriate chemotherapy. Early diagnosis and prompt treatment may improve a patient's prognosis. (*Circ J* 2005; **69:** 243–245)

Key Words: Acquired immunodeficiency syndrome; Chemotherapy; Lymphoma

Acquired immunodeficiency syndrome (AIDS) has been gradually become a worldwide pandemic. The most common early manifestations of human immunodeficiency virus (HIV) infection are signs of viremia such as fever and pharyngitis, and diseases involving the cardiovascular system are rare. Generally, cardiac complications tend to appear later in the course. We present a case of cardiac tumor that was the patient's first manifestation of AIDS.

Case Report

A woman in her 30s was admitted to hospital for investigation and treatment of a mass in her right atrium, detected out at a local hospital. She had a high fever (38°C) and complained of general fatigue and dyspnea on effort that had lasted for 2 weeks. Her blood pressure was 112/80 mmHg and pulse rate was 126 beats/min. She did not have significant skin lesions or lymphadenopathy. On auscultation, no significant heart murmur was heard, but diminished breathing sounds and coarse rales were noted at the base of the right lung. The liver was palpable with 3-finger breadth beneath the right costal margin. Her ECG revealed sinus tachycardia and the QRS axis showed right axis deviation. A chest roentgenogram demonstrated a right-sided pleural effusion and mildly enlarged cardiac silhouette with a cardiothoracic ratio of 0.56. Two-dimensional echocardiography showed a relatively small left ventricle (diastolic diameter, 44 mm and systolic diameter, 30 mm) with normal wall motion. However, we found a large echogenic mass (53×35 mm) in the right atrium, virtually obstructing the tricuspid valve orifice at mid-diastole. The estimated peak pressure gradient between the right atrium and ventricle from the mild tricuspid regurgitation was 18 mmHg, indicating the absence of pulmonary hypertension. A small pericardial effusion was present without signs of pericardial tamponade. The mass did not invade the inferior and superior vena cavae (Fig 1).

Although her leukocyte count was 5,960/mm^3, an elevated erythrocyte sedimentation rate (130 mm/h) and increased C-reactive protein (5.96 mg/dl, normal <0.3) suggested inflammation. Lactate dehydrogenase was 691 IU/ml (normal 100–225). The soluble-interleukin 2 receptor was 4,290 U/ml (normal 145–519) and interleukin 6 was 36.5 pg/ml (normal <4.0). Because of the likelihood of surgery for the right atrial mass, we checked for the presence or absence of various infections with her consent and found that the anti HIV antibody was positive. Her CD4 count was 58/mm^3 (normal >800), which suggested that she was in a state of severe immunodeficiency caused by HIV infection.

To investigate lesions related to the HIV infection, we performed whole-body computed tomography (CT). Plain CT scan revealed pleural effusion and pulmonary embolism and contrast-enhanced CT showed a large mass in the right atrium. The CT scan also demonstrated hepatomegaly with several intrahepatic low density areas, a large mass in the right renal pelvis and para-aortic lymphadenopathy. Magnetic resonance imaging (MRI) revealed a large right atrial mass that was homogeneous but had several bunches.

(Received August 19, 2003; revised manuscript received January 16, 2004; accepted February 6, 2004)

*Departments of Cardiology and *Radiology, National Cardiovascular Center, Suita, Departments of †Cardiology and ‡Immunological and Infectious Diseases, National Osaka Hospital, Osaka, Japan*
Mailing address: Satoshi Nakatani, MD, Department of Cardiology, National Cardiovascular Center, 5-7-1 Fujishiro-dai, Suita 565-8565, Japan. E-mail: nakatas@hsp.ncvc.go.jp

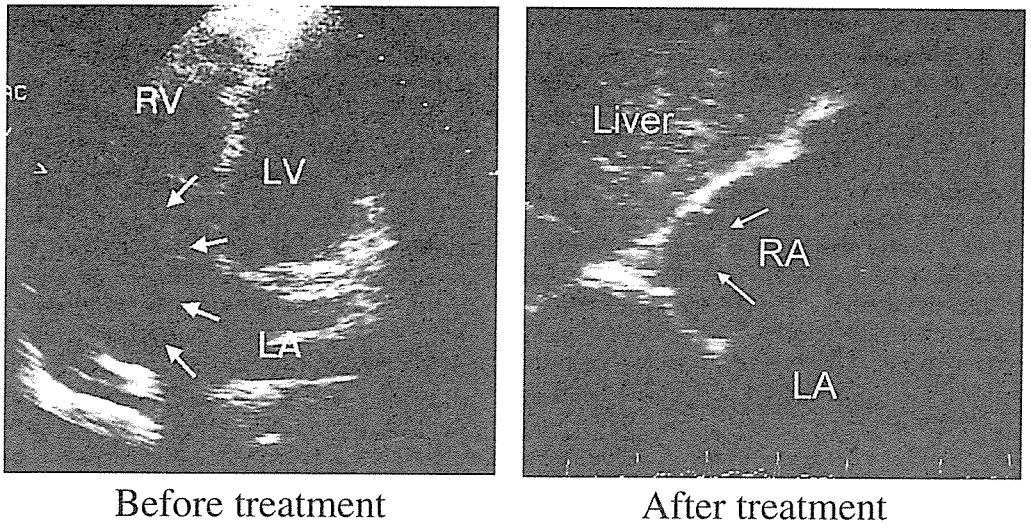

Fig 1. Echocardiography before (Left) and after chemotherapy (Right). Before treatment, the apical 4-chamber view shows a huge mass in the right atrium (arrows). After treatment, the subcostal view shows shrinkage of the mass (arrows). LA, left atrium; LV, left ventricle; RA, right atrium.

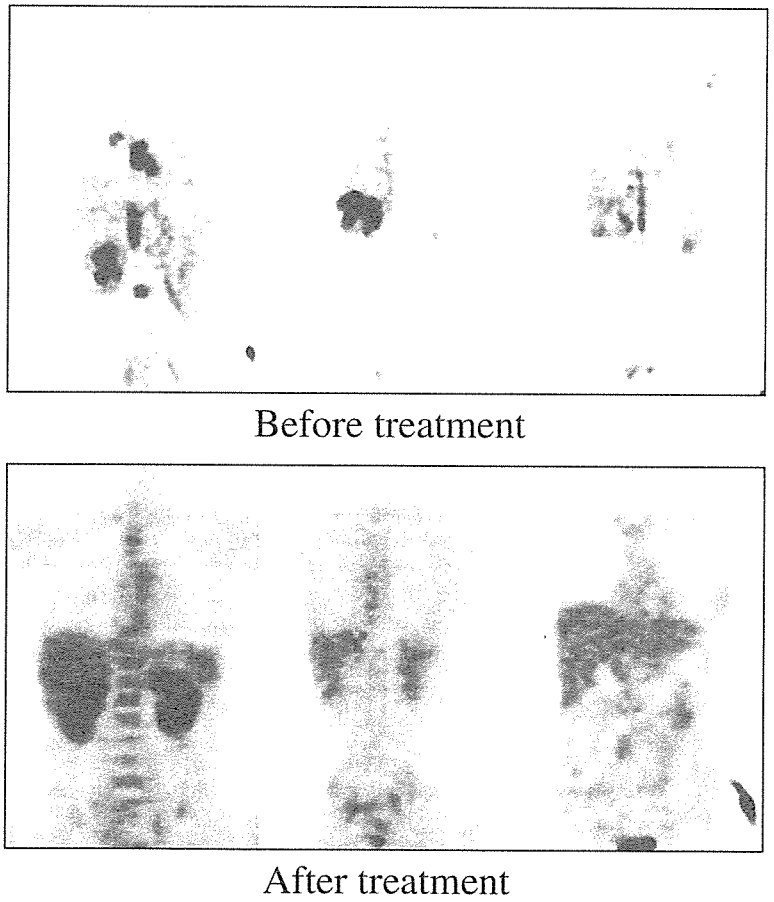

Fig 2. FDG-PET before (Upper) and after chemotherapy (Lower). Before treatment, there was highly dense uptake in the multiple lesions, including the right atrial mass, but after treatment, there was no positive uptake.

It was adhered to the lower atrial septum around the coronary sinus. There was a mass invading the thoracic vertebrae, causing narrowing of the spinal canal and compressing the spinal cord. Another mass was found in the right lower lung. ^{18}F-fluorodeoxyglucose (FDG) -positron emission tomography (PET) showed highly dense uptake in the multiple lesions, including the right atrial mass (Fig 2). These multiple systemic extra-nodal lesions strongly suggested malignant lymphoma secondary to AIDS. Biopsy was not undertaken because of her worsening general condition.

Two days after admission, she began to complain of back pain and the next day she had paresthesia in her lower extremities, which worsened and was considered to be caused by the spinal cord compression. She was transferred to another hospital for chemotherapy and radiation therapy.

Pleural fluid sample was taken there and its cytology was consistent with high-grade B-cell type malignant lymphoma. It later proved to be CD20 positive. She then had 6 cycles of rituximab–cyclophosphamide–vincristine–doxorubicine–predonisolone (R-CHOP) in addition to regular treatment for AIDS. After 1 cycle, her general condition became better allowing a catheter biopsy of the right atrial tumor to be performed. Histopathology of the tumor showed granuloma with inflammatory cells, which was negative for neoplastic cells, possibly reflecting effective R-CHOP therapy. After 6 cycles, she was in complete remission and she could walk with crutches. The HIV load decreased from a baseline volume of 610,000 copies/ml to 100 copies/ml after treatment. The soluble-interleukin 2 receptor decreased to 1,110 U/ml after 6 cycles of treatment and the CD4 count was 50/mm^3. Two-dimensional echocardiography showed a mass still in the right atrium but had dramatically reduced in size (10×10 mm) (Fig 1). Cardiac size (diastolic diameter, 43 mm and systolic diameter, 31 mm) and function did not change substantially. There was neither tricuspid regurgitation nor pericardial effusion and plain CT scan showed neither pleural effusion nor pulmonary embolism. The extracardiac masses initially shown by contrast enhanced CT and MRI had all disappeared. FDG-PET showed no positive uptake on whole-body imaging (Fig 2). Nine months later, she was free of symptoms without any anticoagulant or anti-arrhythmic treatment.

Discussion

AIDS-related non-Hodgkin's cardiac lymphoma as the first manifestation of cardiac involvement is rare[1–4] because the usual prognosis of AIDS with cardiac involvement is extremely poor, even with drastic multiagent chemotherapy![1,5] In the present case, the tumor was associated with the concurrent HIV infection early after admission enabling prompt initiation of appropriate chemotherapy.

Histological confirmation of the right atrial tumor was not available in this case, but we strongly suspected malignant lymphoma based on the results of imaging. MRI detected the multiple extracardiac lesions as well as the cardiac lesion and FDG-PET detected the widespread inflammation. FDG-PET has been reported as approximately 10% more sensitive than conventional CT and low-dose gallium scintigraphy for extranodal staging of lymphoma has a sensitivity of 95–100% and specificity of 97%[6] Echocardiography, which initially detected the cardiac tumor, was useful for monitoring at the bedside the changes in response to treatment. Thorough cardiac examination using echocardiography is thus essential for HIV infected patients.

AIDS-related extranodal lymphoma is most often B-cell type, and 90% of B-cell type lymphoma has CD20. Rituximab has been reported to be effective for CD20-positive AIDS-related non-Hodgkin lymphoma (NHL)![7,8] In the present case, the multiple extracardiac involvement suggested that she was in the critical stage of malignant lymphoma. Further, staging of the lymphoma and her neurological symptoms necessitated immediate chemotherapy and therefore, although only the pleural fluid cytology suggested CD20-positive malignant lymphoma, rituximab was used. It has been reported that the addition of rituximab to the CHOP regimen increases the complete response rate and improves the event-free and overall survival at 2 years without a significant increase in toxic effects[9] Recently, Spina et al have strongly recommended the combination of rituximab plus chemotherapy as the frontline treatment for patients with CD20-positive high-grade NHL and HIV infection![10] Although no previous report has shown that R-CHOP reduces the size of an AIDS-related cardiac lymphoma, we found that R-CHOP and HAART (highly-active-antiretroviral therapy) successfully reduced the size of the tumor and decreased the HIV load. R-CHOP may provide longer survival than CHOP in patients with this type of cardiac involvement.

There have been only a few cases of a cardiac tumor as an initial manifestation of HIV infection, but the present case shows that HIV infection should be considered as a differential diagnosis![11] The incidence of NHL in patients with AIDS is increasing and is estimated to be 25–60 times more than expected in the general population[2] Generally the prognosis of AIDS-related non-Hodgkin's cardiac lymphoma is extremely poor![1–3,10] but we found that R-CHOP and HAART successfully reduced the size of the tumor and decreased the HIV load. Early detection using echocardiography and diagnosis should improve a patient's prognosis.

Acknowledgments

This study was supported in part by the Research Grant for Cardiovascular Diseases from the Ministry of Health, Labor and Welfare of Japan, Tokyo, Japan.

We thank Mr Patrick Davis for assistance with the preparation of the manuscript.

References

1. Barbaro G, Klatt EC. HIV infection and the cardiovascular system. *AIDS Rev* 2002; **4:** 93–103.
2. Duong M, Dubois C, Buisson M, Eicher JC, Grappin M, Chavanet P, et al. Non-Hodgkin's lymphoma of the heart in patients infected with human immunodeficiency virus. *Clin Cardiol* 1997; **20:** 497–502.
3. Rerkpattanapipat P, Wongpraparut N, Jacobs LE, Kotler MN. Cardiac manifestation of acquired immunodeficiency syndrome. *Arch Intern Med* 2000; **160:** 602–608.
4. Imanaka K, Takamoto S, Kimura S, Morisawa Y, Ohtsuka T, Suematsu Y, et al. Coronary artery bypass grafting in a patient with human immunodeficiency virus. *Jpn Circ J* 1999; **63:** 423–424.
5. Toko H, Terasaki F, Kawakami Y, Hayashi T, Suwa M, Hirota Y, et al. A case of malignant lymphoma with diastolic heart failure. *Jpn Circ J* 1998; **62:** 863–867.
6. Reske SN, Buchmann I. Lymphoma. *In*: Richard LW, Henry NW, Russel HM, editors. Principles and practice of positron emission tomography, Philadelphia: Lippincott Williams & Wilkins; 2002; 177–183.
7. Ratner L, Lee J, Tang S, Redden D, Hamzeh F, Herndier B, et al. Chemotherapy for human immunodeficiency virus-associated non-Hodgkin's lymphoma in combination with highly active antiretroviral therapy. *J Clin Oncol* 2001; **19:** 2171–2178.
8. Golay J, Graminga R, Facchinetti V, Capello D, Gaidano G, Introna M. Acquired immunodeficiency syndrome-associated lymphomas are efficiently lysed through complement-dependent cytotoxicity and antibody-dependent cellular cytotoxicity by rituximab. *Br J Haematol* 2002; **119:** 923–929.
9. Coiffier B, Lepage E, Briere J, Herbrecht R, Tilly H, Bouabdallah R, et al. CHOP chemotherapy plus rituximab compared with CHOP alone in elderly patients with diffuse large B-call lymphoma. *N Engl J Med* 2002; **346:** 235–242.
10 Spina M, Sparano JA, Jaeger U, Rossi G, Tirelli U. Rituximab and chemotherapy is highly effective in patients with CD20-positive non-Hodgikin's lymphoma. *AIDS* 2003; **17:** 137–138.
11. Yuda S, Nakatani S, Yutani C, Yamagishi M, Kitamura S, Miyatake K. Trends in the clinical and morphological characteristics of cardiac myxoma. *Circ J* 2002; **66:** 1008–1013.

Ablation of MEK Kinase 1 Suppresses Intimal Hyperplasia by Impairing Smooth Muscle Cell Migration and Urokinase Plasminogen Activator Expression in a Mouse Blood-Flow Cessation Model

Yan Li, MD, PhD*; Tetsuo Minamino, MD, PhD*; Osamu Tsukamoto, MD*; Toshiaki Yujiri, MD, PhD; Yasunori Shintani, MD; Ken-ichiro Okada, MD; Yoko Nagamachi, BS; Masashi Fujita, MD; Akio Hirata, MD; Shoji Sanada, MD, PhD; Hiroshi Asanuma, MD, PhD; Seiji Takashima, MD, PhD; Masatsugu Hori, MD, PhD; Gary L. Johnson, PhD; Masafumi Kitakaze, MD, PhD

Background—Migration, proliferation, and matrix-degrading protease expression of smooth muscle cells (SMCs) are major features of intimal hyperplasia after vascular injury. Although MEK kinase 1 (MEKK1) has been shown to regulate cell migration and urokinase plasminogen activator (uPA) expression, the precise role of MEKK1 in this process remains unknown.

Methods and Results—We triggered a vascular remodeling model by complete ligation of the right common carotid artery in wild-type (WT) and MEKK1-null ($MEKK1^{-/-}$) mice. The intimal areas 28 days after ligation were significantly decreased in the ligated $MEKK1^{-/-}$ arteries compared with WT arteries (28 ± 8 versus 65 ± 17 μm^2, $P<0.05$). There were no differences in the ratios of proliferating cell nuclear antigen (PCNA)–positive cells to total cells within the arterial wall between WT and $MEKK1^{-/-}$ arteries. Proliferation capacity also did not differ between WT and $MEKK1^{-/-}$ cultured aortic smooth muscle cells (AoSMCs). In contrast, the number of intimal PCNA-positive cells 7 days after ligation was significantly smaller in $MEKK1^{-/-}$ arteries. Three different migration assays revealed that migration and invasion of $MEKK1^{-/-}$ AoSMCs were markedly impaired. Addition of full-length MEKK1 restored the migration capacity of $MEKK1^{-/-}$ AoSMCs. The number of $MEKK1^{-/-}$ AoSMCs showing lamellipodia formation by epithelial growth factor was significantly smaller compared with those of WT SMCs. Furthermore, uPA expression after ligation was markedly decreased in $MEKK1^{-/-}$ arteries.

Conclusions—MEKK1 is implicated in vascular remodeling after blood-flow cessation by regulating the migration and uPA expression of SMCs. MEKK1 is a potential target for drug development to prevent vascular remodeling. (***Circulation.* 2005;111:1672-1678.**)

Key Words: remodeling ■ muscle, smooth ■ vasculature ■ restenosis

Blood vessels respond to damaging stimuli by activating a remodeling mechanism that leads to intimal hyperplasia.[1,2] Accumulating evidence has shown that the underlying causes of intimal hyperplasia are the invasion and proliferation of vascular smooth muscle cells (SMCs), both of which processes are triggered and controlled by numerous growth factors and mitogens.[2] Cell invasion involves migration by cytoskeletal reorganization[3] and activation of a cascade of proteases that degrade various extracellular matrix (ECM) components.[2] Urokinase-type plasminogen activator (uPA) is responsible for degradation of the ECM.[4] Recent studies in uPA-deficient mice have demonstrated that the number of neointimal SMCs after injury is markedly reduced compared with those in wild-type (WT) mice, suggesting that uPA plays a critical role in cell invasion during vascular remodeling.[5]

MEK kinase 1 (MEKK1) is a 196-kDa, mitogen-activated protein kinase kinase kinase (MAP3K) that acts as an upstream regulator of several MAPK pathways.[6–8] MEKK1 has been implicated in diverse and cell type–specific biological responses, including cardiac hypertrophy,[6] cell survival,[7]

Received August 26, 2004; revision received November 16, 2004; accepted November 18, 2004.

From the Department of Internal Medicine and Therapeutics (Y.L., T.M., O.T., Y.S., K.-i.O., Y.N., M.F., A.H., S.S., H.A., S.T., M.H.), Osaka University Graduate School of Medicine, Suita, Osaka, Japan; the Department of Cardiovascular Medicine (M.K.), National Cardiovascular Center, Suita, Osaka, Japan; the Department of Cardiology (Y.L.), Xijing Hospital, Forth Military Medical University, Xi'an, People's Republic of China; the Department of Bio-Signal Analysis (T.Y.), Yamaguchi University Graduate School of Medicine, Ube, Yamaguchi, Japan; and the Department of Pharmacology (G.L.J.), University of North Carolina School of Medicine, Chapel Hill, NC.

*Drs Li, Minamino, and Tsukamoto contributed equally to this work.

Correspondence to Tetsuo Minamino, MD, PhD, Division of Cardiology, Department of Internal Medicine and Therapeutics, Osaka University Graduate School of Medicine, 2-2 Yamadaoka, Suita, Osaka 565-0871, Japan. E-mail minamino@medone.med.osaka-u.ac.jp

Circulation is available at http://www.circulationaha.org

DOI: 10.1161/01.CIR.0000160350.20810.0F

and apoptosis.[8] Recent studies on MEKK1-null ($MEKK1^{-/-}$) mice have uncovered a unique function for this protein kinase in cell migration.[9,10] $MEKK1^{-/-}$ mice were found to exhibit impairment of embryonic eyelid closure, a process involving epithelial cell migration.[9] MEKK1 is also involved in growth factor–induced embryonic stem cell migration and contributes to fibroblast and epithelial cell migration in vitro.[10] Furthermore, endogenous and overexpressed MEKK1 was reported to colocalize with the α-actinin cytoskeleton along actin stress fibers in focal adhesions.[11] Conversely, cytoskeletal reorganization can also lead to MEKK1 activation.[12] This close relationship between MEKK1 and the cytoskeleton implies that MEKK1 may be essential for regulating morphological changes such as the formation of lamellipodia, which proceeds to cell migration.[3,13,14] Furthermore, MEKK1 is necessary for uPA upregulation in response to fibroblast growth factor-2 (FGF-2).[15] These findings indicate that MEKK1 might play an important role in SMC migration and uPA production, both of which will affect SMC invasion during vascular remodeling. Herein, using a blood-flow cessation model in mice with targeted ablation of the *MEKK1* gene, we tested our hypothesis that MEKK1 plays a pivotal pathophysiological role in arterial remodeling by regulating SMC migration and uPA expression.

Methods

Animals and Blood-Flow Cessation Model

All animal studies were conducted in accordance with guidelines of the National Institutes of Health (Bethesda, Md) and institutional Animal Care and Use Committees. $MEKK1^{-/-}$ mice were generated as described previously.[9] The blood-flow cessation model was performed as reported previously.[16] Carotid arteries were harvested immediately for biochemical analysis or after fixation for morphological and immunohistological analysis 1, 3, 7, and 28 days after surgery.

Morphometric and Histological Examinations

Standard hematoxylin-eosin staining, elastica van Gieson's staining, immunostaining for uPA (1:100, American Diagnostica), and proliferating cell nuclear antigen (PCNA) staining (1:50, Santa Cruz) were performed on serial sections (5 μm) within 0.5 mm proximal to the site of ligation of right common carotid arteries, as reported previously.[17,18] The luminal, internal elastic lamina (IEL), and external elastic lamina areas were measured with Scion Image software (Scion Corp). Morphological parameters were calculated as described previously.[19] In brief, the intimal area was calculated as the IEL area minus luminal area, and the medial area was the external elastic lamina area minus IEL area. The ratio of intima to media area (I/M) was calculated as intimal area/medial area, and the stenotic ratio was calculated as the intimal area/IEL area×100.

Primary Culture of AoSMCs and Transfection

Primary culture of aortic SMCs (AoSMCs) was performed and characterized as described previously.[20] Cells were identified by positive immunostaining for α-smooth muscle actin (American Research Products). AoSMCs were transiently transfected with lipofectamine and either a full-length form of MEKK1 vector (MEKK1FL) or an empty vector (pcDNA3.1).[21] After 48 hours, SMCs were studied in migration assays or for uPA expression.

AoSMC Proliferation Assay

AoSMCs (5×10^3) were cultured for 24 hours in 96-well plates with or without epithelial growth factor (EGF, 20 ng/mL), FGF-2 (20 ng/mL, R&D Systems, Inc), or platelet-derived growth factor-BB (PDGF-BB, 25 ng/mL, Sigma). Then, [^{3}H]thymidine incorporation and cell number were measured, as previously reported.[22]

Quantification of Scrape Wound–Induced Migration Assay

Dense monolayers of overconfluent AoSMCs grown on Laboratory-Tek chamber slides were scraped with a sterile scraper as described previously.[23] After the wound was created, cells were incubated for 24 hours with or without FGF-2 (20 ng/mL) and visualized with rhodamine-phalloidin (R-451, Molecular Probes). The number of and distance that AoSMCs migrated from the wound line were calculated as the mean of 6 different fields.

Aortic Explant Migration Assay

Preparation of aortic explants was performed as described previously.[24] Explants were counted as positive when >1 cell was observed and identified by positive staining for α-smooth muscle actin.

Transwell Matrigel-Coated Chamber Invasion Assay

Cell invasion was analyzed with a BioCoat Matrigel invasion chamber (BD Biosciences Corp), as described previously.[25] Inserts without a Matrigel coating were used as controls. FGF-2 (20 ng/mL) was added to the lower chambers as a chemoattractant. The number of invading cells was manually counted per high-power field for each condition (10 fields for each filter). The percentage of invasion was calculated as (invading cells in Matrigel inserts/migrated cells of control inserts) × 100.

Immunofluorescence Confocal Microscopy

Immunofluorescence staining with rhodamine-phalloidin and a monoclonal antibody for uPA (1:50) was performed as described previously.[26] Staining was examined with a Nikon Eclipase TE2000-U confocal scanning electron microscope.

Protein Extraction and Western Blotting Analysis

Protein extraction and immunoblotting were performed as described previously.[15,21,22] Protein phosphorylation levels were normalized to the matching densitometric values of nonphosphorylated proteins.

Statistical Analysis

All data were expressed as mean±SEM. Significant differences were analyzed by an unpaired Student *t* test, Fisher exact test, or ANOVA followed by the Bonferroni post hoc test. A value of $P<0.05$ was considered statistically significant.

Results

MEKK1 Ablation Inhibits Intimal Hyperplasia

There was no intimal thickening in unligated arteries of either WT or $MEKK1^{-/-}$ mice. Significant neointimal growth was observed 28 days after ligation in WT mice, whereas it was much less in $MEKK1^{-/-}$ mice (Figure 1A). Morphometric analysis of ligated arteries on day 28 revealed that the average intimal area was significantly smaller in $MEKK1^{-/-}$ mice than in WT mice, whereas no difference in medial area was observed between WT and $MEKK1^{-/-}$ mice (Figure 1B). Consequently, I-M ratios and stenotic ratios were significantly decreased in $MEKK1^{-/-}$ mice compared with those in WT mice (Figure 1B).

MEKK1 Ablation Prevented Increases in the Numbers of Intimal PCNA-Positive Cells

In both WT and $MEKK1^{-/-}$ mice, the ratios of PCNA-positive cells to total cells within the arterial wall, intima, and media were significantly increased 3 days after ligation

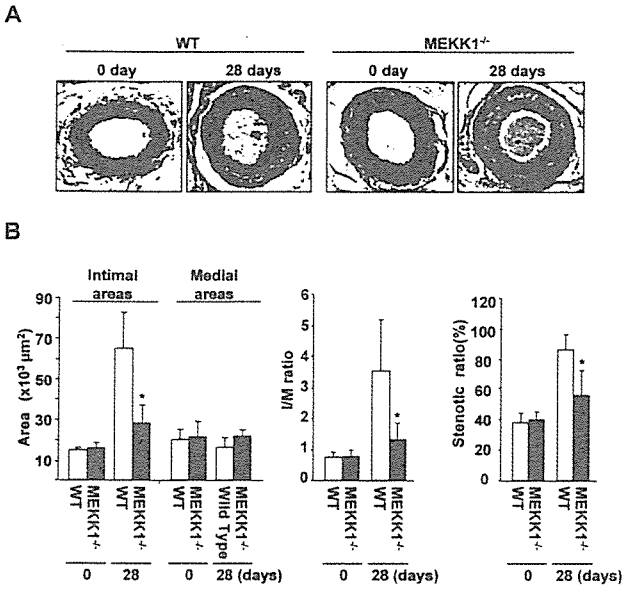

Figure 1. Photomicrographs and morphometry of intimal formation after ligation of carotid arteries. A, Representative cross sections of unligated and ligated carotid arteries on day 28 (elastica van Gieson's stain). Bar indicates 100 μm. B, Quantitative analysis of intimal and medial areas, I-M ratio, and stenotic ratio of ligated arteries. *$P<0.05$ vs WT mice.

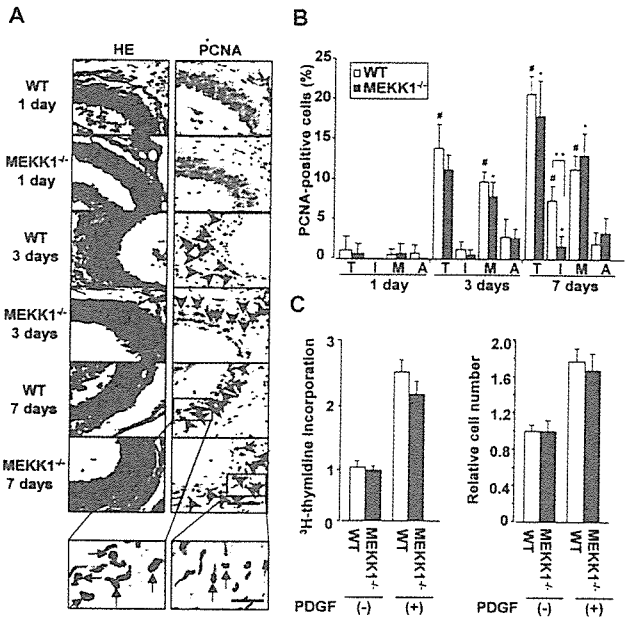

Figure 2. Effects of ablation of MEKK1 on cell proliferation. A, Immunohistochemical analysis of hematoxylin and eosin staining and PCNA staining 1, 3, and 7 days after ligation. Bar indicates 100 μm. Photographs of WT and MEKK1$^{-/-}$ mice 7 days after ligation were enlarged, and bar indicates 30 μm. Red arrowheads indicate PNCA-positive cells. B, Quantification of ratio of PCNA-positive cells to total cell number in arterial wall (T), intima (I), media (M), and adventitia (A) of ligated arteries at 1, 3, and 7 days. Black bars and white bars indicate WT and MEKK1$^{-/-}$ mice, respectively. #$P<0.05$ vs day 1 in WT mice; *$P<0.05$ vs day 1 in MEKK1$^{-/-}$ mice; **$P<0.05$ vs day 7 in WT mice. C, Effects of MEKK1 on PDGF-BB–induced [^{3}H]thymidine incorporation and cell number in AoSMCs. Data are indicated as percentages relative to control group and are mean±SEM of 10 wells in each group of at least 3 replicates.

compared with those 1 day after ligation, but there were no significant differences between WT and MEKK1$^{-/-}$ mice. It is noteworthy that 7 days after ligation, the number of PCNA-positive cells in the intima was significantly less in MEKK1$^{-/-}$ arteries than in WT arteries, although there was no difference within other areas (Figure 2A and 2B). These findings suggest that migration of PCNA-positive cells from the media to the intima was impaired, whereas proliferation was not impaired in MEKK1$^{-/-}$ mice. Consistent with in vivo data, no difference was observed in [^{3}H]thymidine incorporation and cell number between WT and MEKK1$^{-/-}$ AoSMCs after stimulation with PDGF-BB in vitro (Figure 2C). Treatment with EGF or FGF-2 instead of PDGF-BB yielded identical results (data not shown).

Effects of Ablation of MEKK1 on MAPK Activities of AoSMCs

Ablation of MEKK1 does not affect the total protein expression of extracellular signal–regulated kinase (ERK), c-Jun NH_2-terminal kinase (JNK), or p38. We examined the effects of ablation of MEKK1 on MAPK activities of AoSMCs. FGF-2–induced JNK and ERK but not p38 activation in AoSMCs from MEKK1$^{-/-}$ mice was less than that from WT mice (Figure 3A). We confirmed that addition of MEKK1 restored MEKK1 protein levels in MEKK1$^{-/-}$ AoSMCs (Figure 3B). Addition of MEKK1 restored JNK and ERK activation in response to FGF-2 in MEKK1$^{-/-}$ AoSMCs (Figure 3C and 3D). Treatment with EGF or PDGF-BB instead of FGF-2 yielded identical results (data not shown).

MEKK1 Ablation Inhibited AoSMC Migration and Invasion

In the scrape wound–induced migration assays, the average number of and distance that MEKK1$^{-/-}$ AoSMCs migrated from the wound edge (white dotted line) in the absence of any stimulus was similar to those in WT mice; however, the FGF-2–induced increase in cell number and distance was significantly suppressed in MEKK1$^{-/-}$ AoSMCs compared with WT cells. Addition of MEKK1 restored the number and distance of MEKK1$^{-/-}$ AoSMCs to normal levels (Figure 4A and 4B).

In the aortic explant assays, the number of AoSMCs migrating from MEKK1$^{-/-}$ explants at 10 days was considerably lower than those from WT explants (Figure 4C). Moreover, the number of MEKK1$^{-/-}$ aortic explants that showed migrating cells was significantly smaller than in WT explants (27.2±2.2% versus 60.0±2.5%, $P<0.05$).

In the transwell Matrigel-coated chamber invasion assays, the number of invading MEKK1$^{-/-}$ AoSMCs in response to FGF-2 was suppressed markedly compared with WT cells. Addition of MEKK1 restored the number of MEKK1$^{-/-}$ AoSMCs to normal levels (Figure 4D). Treatment with EGF or PDGF-BB instead of FGF-2 yielded identical results (data not shown).

MEKK1 Ablation Impaired Lamellipodia Formation

There were no morphological differences between WT and MEKK1$^{-/-}$ AoSMCs under basal conditions; however, typi-

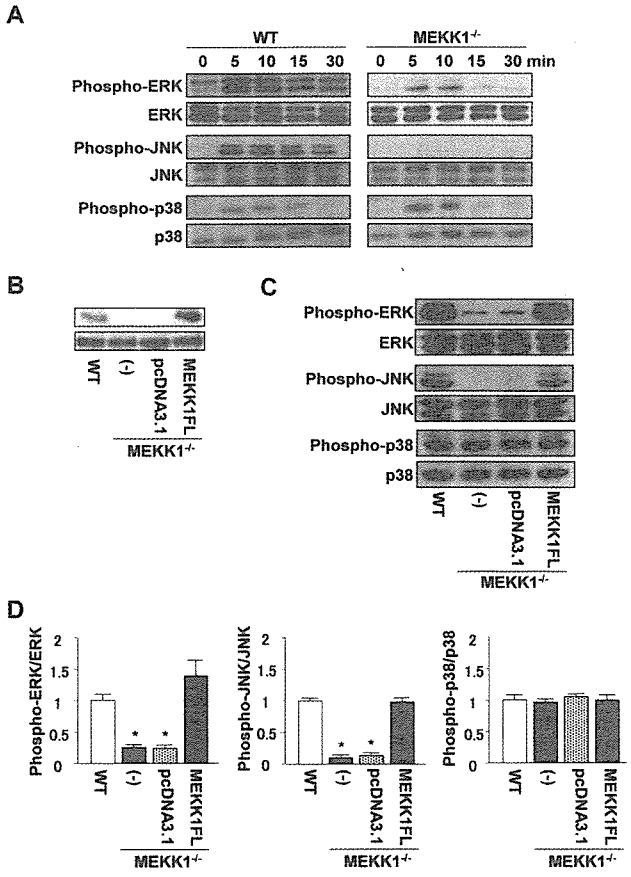

Figure 3. Effects of ablation of MEKK1 on MAPK activities in AoSMCs. A, Time course of JNK, ERK, and p38 activities followed by FGF-2 stimulation. B, Addition of MEKK1 experiments in MEKK1$^{-/-}$ AoSMCs. C, Western blot analysis of MAPKs in MEKK1$^{-/-}$ AoSMCs transfected with empty vector (pcDNA3.1) or full-length forms of MEKK1 vector (MEKK1FL) followed by FGF-2 stimulation. D, Cumulative data for MAPK in Figure 3C. *P<0.05 vs WT AoSMCs.

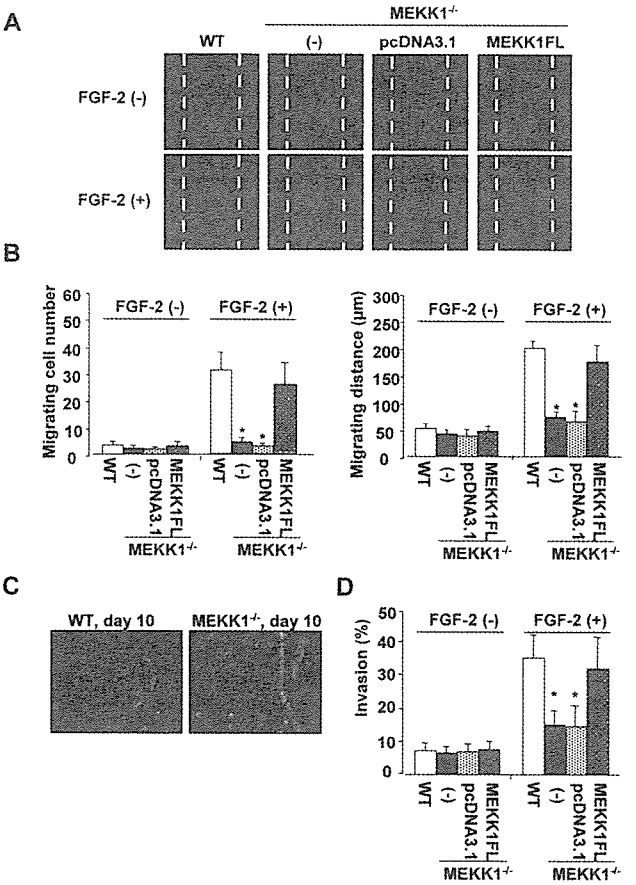

Figure 4. Migration and invasion of AoSMCs. A, Scrape wound–induced migration assay. Immunofluorescence microscopy of migrating cells from wound edge when AoSMCs were cultured for 24 hours with or without FGF-2. F-actin was stained with rhodamine-phalloidin (red), and nuclei were counterstained with DAPI (blue; not visible). B, Quantification of means of number and distance of migrating cells. *P<0.05 vs WT AoSMCs. C, Migration of AoSMCs from aortic explants on day 10. D, Quantification of percent invasion of AoSMCs by transwell Matrigel-coated chamber invasion assay. *P<0.05 vs WT AoSMCs.

cal lamellipodia formation was induced by treatment with EGF in WT AoSMCs but was seldom induced in MEKK1$^{-/-}$ AoSMCs (Figure 5A). The percentage of MEKK1$^{-/-}$ AoSMCs showing lamellipodia was significantly lower than in WT AoSMCs (P<0.05). Addition of MEKK1 restored the lamellipodia-forming capacity of MEKK1$^{-/-}$ AoSMCs (Figure 5B). Treatment with FGF-2 or PDGF-BB instead of EGF yielded identical results (data not shown).

MEKK1 Ablation Decreased uPA Expression

uPA expression began to increase on day 1 and reached a peak on day 3, after which it decreased gradually by 7 days after ligation in WT mice. In contrast, there was only weak positive staining for uPA up to 7 days in MEKK1$^{-/-}$ mice (Figure 6A). In vitro immunofluorescence staining revealed that PDGF-BB–induced uPA expression was decreased in MEKK1$^{-/-}$ AoSMCs compared with those of WT mice (Figure 6B). Western blotting showed a dramatic reduction of FGF-2–induced uPA expression in MEKK1$^{-/-}$ AoSMCs, which was restored by addition of MEKK1 (Figure 6C).

Discussion

Several lines of evidence suggest that MEKK1 is implicated in diverse biological responses.[6–8] Recently, the unique role of MEKK1 in regulating the migration of several cell types has aroused widespread attention[9,12,27] and inspired us to study its involvement in cardiovascular diseases. Up to now, there has been no previous report on the role of MEKK1 in the development of vascular remodeling, during which invasion and proliferation of SMCs play key roles. In the present study, we investigated the mechanism whereby MEKK1 regulates vascular remodeling in a well-established, blood-flow cessation model in MEKK1$^{-/-}$ mice. We found that MEKK1 is essential for intimal hyperplasia after cessation of blood flow.

In this study, we clearly demonstrated that intimal areas, I-M ratios, and stenotic ratios of the ligated arteries were significantly lower in MEKK1$^{-/-}$ mice relative to WT mice, indicating that MEKK1 is implicated in intimal hyperplasia. Although an angioplasty/balloon injury model would have yielded greater applicability to the clinical situation, we used

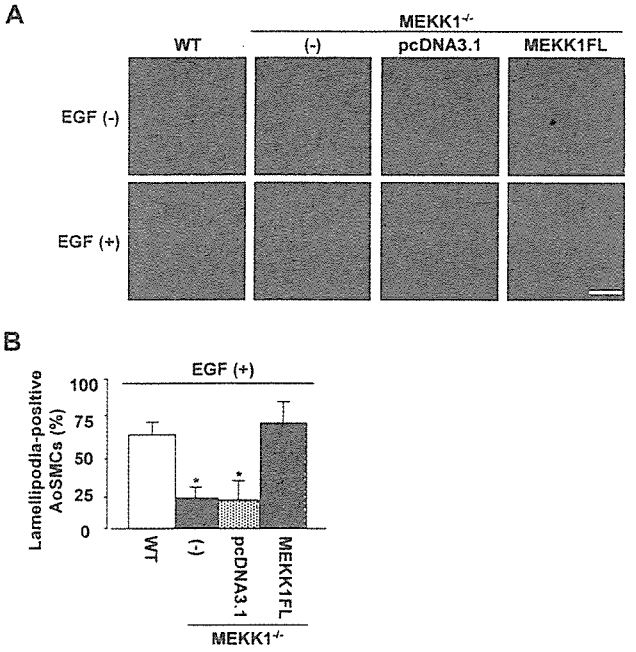

Figure 5. Lamellipodia formation in AoSMCs. A, Representative photomicrographs of lamellipodia formation in AoSMCs with or without EGF stimulation. Bar indicates 25 μm. B, Percentage of lamellipodia-positive cells (n=100) in AoSMCs with EGF. *$P<0.05$ vs WT AoSMCs.

the ligation model because of its excellent reproducibility. To clarify the mechanism(s) of MEKK1 involvement, we first examined cell proliferation within the arterial wall after ligation and found no statistically significant difference in the number of PCNA-positive cells between WT and MEKK1$^{-/-}$ mice. Results from this ligation model are consistent with the fact that MEKK1$^{-/-}$ mice have no overt defects in growth and fertility.[9] There was also no difference in the proliferation of WT and MEKK1$^{-/-}$ AoSMCs evaluated by [^{3}H]thymidine incorporation and cell number. These findings suggest that SMC proliferation might not contribute to the reduced intimal hyperplasia in MEKK1$^{-/-}$ mice. Then we investigated SMC migration and uPA expression, both of which are important factors for intimal hyperplasia.

We demonstrated that there were significantly fewer intimal PCNA-positive cells 7 days after ligation in MEKK1$^{-/-}$ mice than in WT mice. Because PCNA-positive cells are believed to migrate from the media to the intima,[2] this finding suggests that SMC migration is impaired in MEKK1$^{-/-}$ mice. To directly assess the effects of MEKK1 ablation on SMC migration, we used several migration and invasion assays in vitro. We observed comparable migration or invasion of SMCs under control condition between WT and MEKK1$^{-/-}$ AoSMCs; however, significant impairment of migration or invasion was observed after stimulation with FGF-2 in MEKK1$^{-/-}$ AoSMCs, which was restored by addition of full-length MEKK1. These findings indicate that ablation of MEKK1 impairs invasion and migration, both of which may contribute to reduced intimal hyperplasia wherein growth factors may play a vital role.

Lamellipodia formation is essential for cell migration.[13] Exogenous stimuli, such as PDGF or FGF-2, induce lamellipodia formation that can help to complete the first step of the motility cycle.[14,28] Therefore, we examined whether MEKK1 is involved in lamellipodia formation in AoSMCs. Our results showed that the percentage of lamellipodia-positive cells was significantly smaller in MEKK1$^{-/-}$ AoSMCs compared with WT AoSMCs in the presence of EGF. This finding suggests that the impairment of migration in MEKK1$^{-/-}$ AoSMCs may be due to inhibited formation of lamellipodia. Indeed, addition of MEKK1 to MEKK1$^{-/-}$ AoSMCs recovered their capacity to form lamellipodia and migrate. On the other hand, it has been reported that loss of MEKK1 disrupts focal adhesion composition, with decreased vinculin content and focal adhesion kinase (FAK) cleavage.[29] Because disruption of focal adhesion composition will affect cell migration, further investigation will be needed to clarify its role in MEKK1$^{-/-}$ mice.

There is evidence that uPA is induced after arterial injury.[5,28,30,31] uPA enhances vascular remodeling by transforming plasminogen into plasmin, which can activate metalloproteinases and in turn degrade ECM proteins.[5,30,31] We found that uPA expression began to increase at 1 day and reached a peak 3 days after ligation in WT mice, whereas uPA staining appeared to be significantly lower in MEKK1$^{-/-}$ arteries at corresponding times. In vitro, PDGF-BB– and FGF-2–induced uPA expression as detected by immunofluorescence staining and Western blotting was also significantly decreased in MEKK1$^{-/-}$ AoSMCs. Thus, in addition to impaired lamellipodia formation, inhibited uPA expression by MEKK1 ablation may also contribute to impairment of SMC invasion. Addition of full-length MEKK1 restored uPA expression in MEKK1$^{-/-}$ AoSMCs.

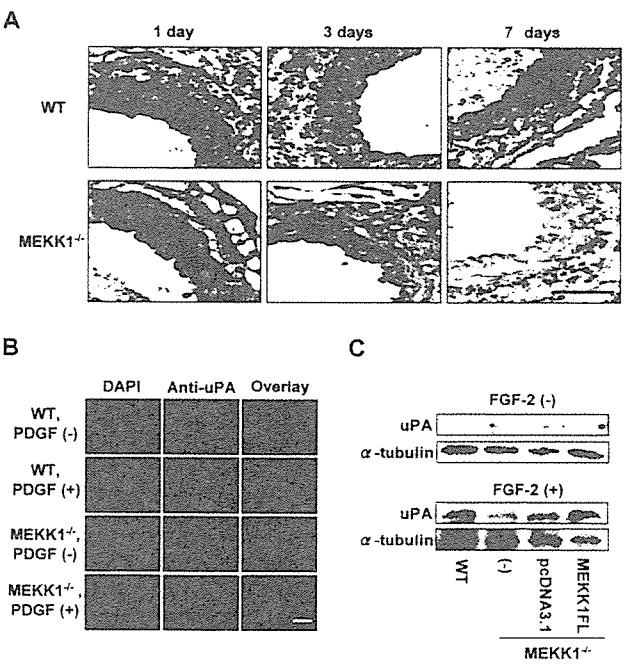

Figure 6. Expression of uPA in AoSMCs. A, Immunohistochemical analysis of time course of uPA expression 1, 3, and 7 days after ligation of carotid arteries. Bar indicates 100 μm. B, Immunofluorescence staining for uPA in AoSMCs stimulated with PDGF-BB. Bar indicates 10 μm. C, Western blots of uPA in AoSMCs stimulated with FGF-2.

Although it has been reported that MEKK1 is required for FGF-2–induced signals to control uPA expression in fibroblasts,[15] further investigations will be needed to elucidate the mechanism by which MEKK1 regulates uPA expression in arteries after ligation.

Recent studies have demonstrated that JNK and ERK transduction pathways may regulate cell migration[32,33] and uPA expression.[34,35] In the present study, we demonstrated that JNK and ERK activation after growth factor stimulation was blunted in MEKK1$^{-/-}$ AoSMCs. Thus, it is possible that ablation of MEKK1 may inhibit cell migration and uPA expression by interfering with the downstream signaling pathways JNK and/or ERK. MEKK1 also has been reported to be associated with cytoskeletal reorganization[11,12] and to be necessary for uPA upregulation,[15] suggesting another possibility that ablation of MEKK1 directly inhibits lamellipodia formation and uPA expression. The stimulus for remodeling after ligation is also influenced by the resultant vascular ischemia. Because MEKK1 is activated by hypoxic stimuli as well as growth factors,[36] we must consider the possibility that the resultant hypoxic stimuli are also important during vascular remodeling in the ligation model.

Izumi et al[22] demonstrated that activation of apoptosis signal–regulating kinase 1 (ASK1), another member of the MAP3K family, also plays a key role during intimal hyperplasia in the carotid artery balloon injury model. Unlike MEKK1, ablation of ASK1 blunted both JNK and p38 but not ERK activation in AoSMCs after serum stimulation. In addition, ablation of ASK1 caused impairment of both SMC migration and proliferation. Thus, although the methods or models used to evaluate functions of MEKK1 and ASK1 were not the same, both MEKK1 and ASK1 may contribute to the development of intimal hyperplasia by different mechanisms.

In conclusion, we have demonstrated that MEKK1 plays a critical role during intimal hyperplasia in a mouse carotid blood-flow cessation model. Intimal hyperplasia is greatly lessened, possibly due to a reduction of SMC invasion by an impairment of their migration and reduced uPA expression. We propose that MEKK1 is a potential target for drug development to prevent vascular remodeling.

Acknowledgments

This study was supported by grants on Human Genome, Tissue Engineering, and Food Biotechnology (H13-genome-11) and grants on Comprehensive Research on Aging and Health [H13-21seiki(seikatsu)-23] in Health and Labor Science Research from the Ministry of Health, Labor, and Welfare, Japan. We thank Hiroko Okuda for technical assistance and Yukari Arino for secretarial work.

References

1. Sakaguchi T, Yan SF, Yan SD, Belov D, Rong LL, Sousa M, Andrassy M, Marso SP, Duda S, Arnold B, Liliensiek B, Nawroth PP, Stern DM, Schmidt AM, Naka Y. Central role of RAGE-dependent neointimal expansion in arterial restenosis. *J Clin Invest.* 2003;111:959–972.
2. Newby AC, Zaltsman AB. Molecular mechanisms in intimal hyperplasia. *J Pathol.* 2000;190:300–309.
3. Maheshwari G, Lauffenburger DA. Deconstructing (and reconstructing) cell migration. *Microsc Res Tech.* 1998;43:358–368.
4. Reidy MA, Irvin C, Lindner V. Migration of arterial wall cells: expression of plasminogen activators and inhibitors in injured rat arteries. *Circ Res.* 1996;78:405–414.
5. Carmeliet P, Moons L, Herbert JM, Crawley J, Lupu F, Lijnen R, Collen D. Urokinase but not tissue plasminogen activator mediates arterial neointima formation in mice. *Circ Res.* 1997;81:829–839.
6. Minamino T, Yujiri T, Terada N, Taffet GE, Michael LH, Johnson GL, Schneider MD. MEKK1 is essential for cardiac hypertrophy and dysfunction induced by Gq. *Proc Natl Acad Sci U S A.* 2002;99:3866–3871.
7. Yujiri T, Sather S, Fanger GR, Johnson GL. Role of MEKK1 in cell survival and activation of JNK and ERK pathways defined by targeted gene disruption. *Science.* 1998;282:1911–1914.
8. Minamino T, Yujiri T, Papst PJ, Chan ED, Johnson GL, Terada N. MEKK1 suppresses oxidative stress–induced apoptosis of embryonic stem cell–derived cardiac myocytes. *Proc Natl Acad Sci U S A.* 1999;96:15127–15132.
9. Yujiri T, Ware M, Widmann C, Oyer R, Russell D, Chan E, Zaitsu Y, Clarke P, Tyler K, Oka Y, Fanger GR, Henson P, Johnson GL. MEK kinase 1 gene disruption alters cell migration and c-Jun NH_2-terminal kinase regulation but does not cause a measurable defect in NF-κB activation. *Proc Natl Acad Sci U S A.* 2000;97:7272–7277.
10. Xia Y, Makris C, Su B, Li E, Yang J, Nemerow GR, Karin M. MEK kinase 1 is critically required for c-Jun *N*-terminal kinase activation by proinflammatory stimuli and growth factor–induced cell migration. *Proc Natl Acad Sci U S A.* 2000;97:5243–5248.
11. Christerson LB, Vanderbilt CA, Cobb MH. MEKK1 interacts with α-actinin and localizes to stress fibers and focal adhesions. *Cell Motil Cytoskeleton.* 1999;43:186–198.
12. Yujiri T, Fanger GR, Garrington TP, Schlesinger TK, Gibson S, Johnson GL. MEK kinase 1 (MEKK1) transduces c-Jun NH_2-terminal kinase activation in response to changes in the microtubule cytoskeleton. *J Biol Chem.* 1999;274:12605–12610.
13. Small JV, Stradal T, Vignal E, Rottner K. The lamellipodium: where motility begins. *Trends Cell Biol.* 2002;12:112–120.
14. DesMarais V, Ichetovkin I, Condeelis J, Hitchcock-DeGregori SE. Spatial regulation of actin dynamics: a tropomyosin-free, actin-rich compartment at the leading edge. *J Cell Sci.* 2002;115:4649–4660.
15. Witowsky J, Abell A, Johnson NL, Johnson GL, Cuevas BD. MEKK1 is required for inducible urokinase-type plasminogen activator expression. *J Biol Chem.* 2003;278:5941–5946.
16. Kumar A, Lindner V. Remodeling with neointima formation in the mouse carotid artery after cessation of blood flow. *Arterioscler Thromb Vasc Biol.* 1997;17:2238–2244.
17. Schafer K, Konstantinides S, Riedel C, Thinnes T, Muller K, Dellas C, Hasenfuss G, Loskutoff DJ. Different mechanisms of increased luminal stenosis after arterial injury in mice deficient for urokinase- or tissue-type plasminogen activator. *Circulation.* 2002;106:1847–1852.
18. Murakoshi N, Miyauchi T, Kakinuma Y, Ohuchi T, Goto K, Yanagisawa M, Yamaguchi I. Vascular endothelin-B receptor system in vivo plays a favorable inhibitory role in vascular remodeling after injury revealed by endothelin-B receptor–knockout mice. *Circulation.* 2002;106:1991–1998.
19. Kuzuya M, Kanda S, Sasaki T, Tamaya-Mori N, Cheng XW, Itoh T, Itohara S, Iguchi A. Deficiency of gelatinase A suppresses smooth muscle cell invasion and development of experimental intimal hyperplasia. *Circulation.* 2003;108:1375–1381.
20. Bradshaw AD, Francki A, Motamed K, Howe C, Sage EH. Primary mesenchymal cells isolated from SPARC-null mice exhibit altered morphology and rates of proliferation. *Mol Biol Cell.* 1999;10:1569–1579.
21. Yujiri T, Nawata R, Takahashi T, Sato Y, Tanizawa Y, Kitamura T, Oka Y. MEK kinase 1 interacts with focal adhesion kinase and regulates insulin receptor substrate-1 expression. *J Biol Chem.* 2003;278:3846–3851.
22. Izumi Y, Kim S, Yoshiyama M, Izumiya Y, Yoshida K, Matsuzawa A, Koyama H, Nishizawa Y, Ichijo H, Yoshikawa J, Iwao H. Activation of apoptosis signal–regulating kinase 1 in injured artery and its critical role in neointimal hyperplasia. *Circulation.* 2003;108:2812–2818.
23. Galis ZS, Johnson C, Godin D, Magid R, Shipley JM, Senior RM, Ivan E. Targeted disruption of the matrix metalloproteinase-9 gene impairs smooth muscle cell migration and geometrical arterial remodeling. *Circ Res.* 2002;91:852–859.
24. Hsieh CC, Lau Y. Migration of vascular smooth muscle cells is enhanced in cultures derived from spontaneously hypertensive rat. *Pflugers Arch.* 1998;435:286–292.

25. Chaulet H, Desgranges C, Renault MA, Dupuch F, Ezan G, Peiretti F, Loirand G, Pacaud P, Gadeau AP. Extracellular nucleotides induce arterial smooth muscle cell migration via osteopontin. *Circ Res.* 2001;89:772–778.
26. Watanabe M, Yano W, Kondo S, Hattori Y, Yamada N, Yanai R, Nishida T. Up-regulation of urokinase-type plasminogen activator in corneal epithelial cells induced by wounding. *Invest Ophthalmol Vis Sci.* 2003;44:3332–3338.
27. Zhang L, Deng M, Kao CW, Kao WW, Xia Y. MEK kinase 1 regulates c-Jun phosphorylation in the control of corneal morphogenesis. *Mol Vis.* 2003;9:584–593.
28. Kessels MM, Engqvist-Goldstein AE, Drubin DG. Association of mouse actin-binding protein 1 (mAbp1/SH3P7), an Src kinase target, with dynamic regions of the cortical actin cytoskeleton in response to Rac1 activation. *Mol Biol Cell.* 2000;11:393–412.
29. Cuevas BD, Abell AN, Witowsky JA, Yujiri T, Johnson NL, Kesavan K, Ware M, Jones PL, Weed SA, DeBiasi RL, Oka Y, Tyler KL, Johnson GL. MEKK1 regulates calpain-dependent proteolysis of focal adhesion proteins for rear-end detachment of migrating fibroblasts. *EMBO J.* 2003;22:3346–3355.
30. Carmeliet P, Moons L, Lijnen R, Baes M, Lemaitre V, Tipping P, Drew A, Eeckhout Y, Shapiro S, Lupu F, Collen D. Urokinase-generated plasmin activates matrix metalloproteinases during aneurysm formation. *Nat Genet.* 1997;17:439–444.
31. Lamfers ML, Lardenoye JH, de Vries MR, Aalders MC, Engelse MA, Grimbergen JM, van Hinsbergh VW, Quax PH. In vivo suppression of restenosis in balloon-injured rat carotid artery by adenovirus-mediated gene transfer of the cell surface-directed plasmin inhibitor ATF.BPTI. *Gene Ther.* 2001;8:534–541.
32. Xia Y, Karin M. The control of cell motility and epithelial morphogenesis by Jun kinases. *Trends Cell Biol.* 2004;14:94–101.
33. Matsubayashi Y, Ebisuya M, Honjoh S, Nishida E. ERK activation propagates in epithelial cell sheets and regulates their migration during wound healing. *Curr Biol.* 2004;14:731–735.
34. Benasciutti E, Pages G, Kenzior O, Folk W, Blasi F, Crippa MP. MAPK and JNK transduction pathways can phosphorylate Sp1 to activate the uPA minimal promoter element and endogenous gene transcription. *Blood.* 2004;104:256–262.
35. Jo M, Thomas KS, O'Donnell DM, Gonias SL. Epidermal growth factor receptor–dependent and –independent cell-signaling pathways originating from the urokinase receptor. *J Biol Chem.* 2003;278:1642–1646.
36. Lee SR, Lo EH. Interactions between p38 mitogen-activated protein kinase and caspase-3 in cerebral endothelial cell death after hypoxia-reoxygenation. *Stroke.* 2003;34:2704–2709.